



5-1997

Design, implementation, and analysis of a wireless local area network

John P. Parsley

Follow this and additional works at: https://trace.tennessee.edu/utk_gradthes

Recommended Citation

Parsley, John P., "Design, implementation, and analysis of a wireless local area network. " Master's Thesis, University of Tennessee, 1997.
https://trace.tennessee.edu/utk_gradthes/7764

This Thesis is brought to you for free and open access by the Graduate School at TRACE: Tennessee Research and Creative Exchange. It has been accepted for inclusion in Masters Theses by an authorized administrator of TRACE: Tennessee Research and Creative Exchange. For more information, please contact trace@utk.edu.

To the Graduate Council:

I am submitting herewith a thesis written by John P. Parsley entitled "Design, implementation, and analysis of a wireless local area network." I have examined the final electronic copy of this thesis for form and content and recommend that it be accepted in partial fulfillment of the requirements for the degree of Master of Science, with a major in Electrical Engineering.

David B. Koch, Major Professor

We have read this thesis and recommend its acceptance:

Accepted for the Council:

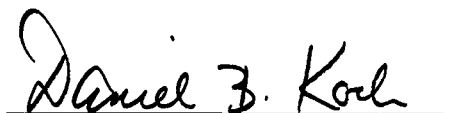
Carolyn R. Hodges

Vice Provost and Dean of the Graduate School

(Original signatures are on file with official student records.)

To the Graduate Council:

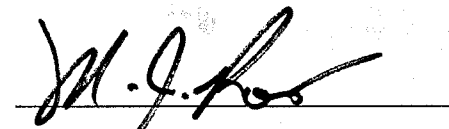
I am submitting herewith a thesis written by John P. Parsley entitled "Design, Implementation, and Analysis of a Wireless Local Area Network." I have examined the final copy of this for form and content and recommend that it be accepted in partial fulfillment of the requirements for the degree of Master of Science, with a major in Electrical Engineering.



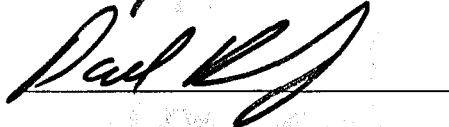
Daniel B. Koch

Daniel B. Koch, Major Professor

We have read this thesis
and recommend its acceptance:



M. J. Koch



Paul R. J.

Accepted for the Council:



Lew Minkal

Associate Vice Chancellor
and Dean of Graduate School

Design, Implementation, and Analysis of a Wireless Local Area Network

A Thesis

Presented for the

Master of Science

Degree

The University of Tennessee, Knoxville

John P. Parsley

May, 1997

To William and Carol Feldhaus

Acknowledgment

Thanks to my major professor, Dr. Daniel B. Koch, whose assistance has made this project a reality. Special thanks to Loeke Brederveld of Lucent Technologies for supplying me with technical information which has been invaluable. Also to Jeffery Parker, Ed Mahon, and Joe Gipson of the University of Tennessee Network Services department for funding the hardware purchases and providing technical assistance.

Thanks also to my mother and step-father Carol and William Feldhaus for their encouragement and support for as long as I can remember, and to Julie for her patience.

Abstract

This thesis is intended to provide information which can be used for further implementation of wireless local area networks on the University of Tennessee campus. By simulating the system of choice and then doing actual field measurements, data was obtained which will simplify future implementation by providing the system designer with information that will minimize the need for further research. The properties of differential quaternary phase shift keying (DQPSK) and direct sequence spread spectrum (DS/SS) modulation are examined as well as multipath interference which greatly effects the performance of an indoor RF system. The protocols used by the wireless LAN system are described as is the procedure used to take performance measurements. Contained within this thesis is an amalgamation of ten months of research, programming, and analysis.

Table of Contents

CHAPTER		PAGE
1.	INTRODUCTION	1
2.	BACKGROUND	4
	2.1 Fundamentals of Wireless Networking	4
	2.2 Current Status of Wireless Networking Possibilities	5
	2.3 The Wireless LAN Project at Carnegie Mellon University	13
	2.4 Standards Efforts	15
	2.5 Product Offerings	19
3.	A MODEL FOR WIRELESS NETWORKING	22
	3.1 Site Selection	22
	3.2 Proposal of an Architecture	24
	3.3 The WavePOINT Access Point	28
	3.4 The WaveLAN PCMCIA Card	30
4.	SIMULATION	32
	4.1 Introduction	32
	4.2 Transmitter/Receiver Characteristics	33
	4.3 Indoor Multipath Channel Characteristics	43
	4.4 System Simulation Description	47
	4.5 Simulation Results	71
5.	FIELD TESTS	78
	5.1 Introduction	78
	5.2 WaveLAN Physical Frame Format	78

5.3	WaveLAN MAC Frame Format	80
5.4	SNAP Frame	82
5.5	The PtPMeasure Protocol	82
5.6	Signal Level and SNR Calculations	86
5.7	Library Architecture	88
5.8	Measurements	90
5.9	Evaluation of Data	99
6.	CONCLUSION	103
	LIST OF REFERENCES	104
	VITA	107

List of Figures

FIGURE		PAGE
2.1	Hybrid wireless/wired LAN	6
2.2	Power spectral density (a) before (b) after spread spectrum modulation	7
2.3	DS/SS transmitter and waveforms	9
2.4	FH/SS modulator	10
2.5	The OSI model	16
3.1	Signal space for DQPSK	26
3.2	Modulation technique for DS/SS	26
3.3	WaveLAN security layers	27
4.1	Block diagram of a differential encoder	34
4.2	Spread Spectrum modulator	36
4.3	Autocorrelation function of an 11-chip Barker Sequence	38
4.4	Spread spectrum demodulator	39
4.5	Block diagram of a DQPSK receiver	41
4.6	Approximate probability of symbol error for DQPSK modulation	44
4.7	Rayleigh pdf	46
4.8	Example of an indoor power delay profile	48
4.9	Block diagram of a spread spectrum DQPSK transmitter	50
4.10	“DIANDDQ” sub-VI	51

4.11	“STREAM” sub-VI	52
4.12	“ENCODE” sub-VI	53
4.13	“GENDQPSK” sub-VI	54
4.14	“BARKER” sub-VI	56
4.15	“MULTIPTS” sub-VI	58
4.16	“RAYLEIGH” sub-VI	59
4.17	“COMPOS” sub-VI	61
4.18	“CHANNEL” sub-VI	62
4.19	Block diagram of a spread spectrum DQPSK receiver	64
4.20	“RECEIVER” sub-VI	65
4.21	“ADDARRAY” sub-VI	66
4.22	“DEMOD” sub-VI	68
4.23	“DECODE” sub-VI	69
4.24	“BITERR” sub-VI	70
4.25	Simulated and theoretical symbol error rates (no multipath interference)	72
4.26	Symbol error rate with 2 paths	73
4.27	Symbol error rate with 5 paths	74
4.28	Symbol error rate with 10 paths	75
4.29	Error performance with and without DS/SS	77
5.1	WaveLAN physical frame format	79
5.2	WaveLAN MAC frame format	81
5.3	SNAP frame structure	83

5.4	PtPMeasure request frames	85
5.5	PtPMeasure response frames	87
5.6	RF modem signal level vs. received level	89
5.7	First floor measurement locations	91
5.8	Second floor measurement locations	92
5.9	Third floor measurement locations	93

List of Tables

TABLE		PAGE
2.1	Summary of wireless LAN access points	21
2.2	Summary of wireless LAN client cards	21
4.1	Symbol assignments	55
5.1	Path loss exponent and standard deviation for various types of buildings	96
5.2	Propagation data for the second floor of Hodges Library	98
5.3	Propagation data for the third floor of Hodges Library	98
5.4	Propagation data for the first floor of Hodges Library	99
5.5	Path loss exponent and standard deviation data for Hodges Library	99

Chapter 1

Introduction

As laptop computers have become commonplace, a need has arisen for the ability to connect them to networks by some means other than a hard-wired connection. Many manufacturers have begun to market both wireless access points and client cards designed especially for this purpose. The access point is a transceiver that is connected to the wired LAN while the client card is plugged into the laptop computer. These devices use RF energy to communicate with each other making two-way data transfer possible. The advantage of using these systems over conventional modems connected to a cellular telephone is that a much higher data transfer rate is possible along with increased reliability.

This thesis project involves the design, implementation, and analysis of a wireless network solution for the University of Tennessee campus. Many students and faculty own laptop computers; however, there is currently no way to access the UTK network when away from a network port or telephone line. Adding fixed network ports to the desired sites on campus is not a practical solution as it would be impossible to install them at every imaginable location where network access is likely to be desired. This approach is also expensive as the cost for copper wire can be as high as \$1,000 per node and may be more for coaxial and fiber optic LANs [1]. A wireless LAN however, could conceivably cover the entire UTK campus (or at least the areas where network access is likely to be needed

such as libraries, classrooms, and conference rooms) while remaining relatively cost effective.

Chapter 2 of this thesis explains the fundamentals of wireless networking and describes the current status of wireless networking possibilities. Most modern wireless systems use some type of spread spectrum modulation. This technique minimizes interference from other users in the same frequency band while also helping to ensure secure communications. Also included in Chapter 2 is a description of existing wireless LANs with an emphasis on the spectrum allocation and protocols currently in use. The IEEE is currently developing a protocol known as 802.11 that will standardize wireless LANs. This protocol is also reviewed in Chapter 2. Finally, Chapter 2 includes information on current product offerings, comparing the price and performance of each.

Chapter 3 discusses the possible sites on the UTK campus for the wireless network based upon the needs of the mobile user. This chapter will include an architecture for the wireless LAN that will be implemented. The selection of frequency band and modulation scheme will also be discussed. Currently, access points and client cards are available that operate in either the 900MHz or 2.4GHz bands. Direct sequence or frequency hopping spread spectrum devices are available that enable seamless roaming between access points. Finally, the hardware and software necessary to implement the system is described in Chapter 3.

A simulation of the wireless LAN was created using LabVIEW. A detailed description of this simulation and the software used to create it is given in Chapter 4. The results from the simulation are also evaluated in this chapter.

Once the wireless system had been installed, field strength and signal to noise ratio (SNR) measurements were taken at various distances from the transmitter while simultaneously measuring error performance. In Chapter 5, these field tests are described. An overview of the equipment and software used to make these measurements is also given. Finally, the results of these field tests are summarized.

In Chapter 6 the results of the simulation and the field tests are compared. Recommendations for improvements to the wireless LAN and future work for continuation of wireless LANs on the University of Tennessee Campus are outlined, and an overview of emerging technologies for wireless LANs is also given.

Chapter 2

Background

2.1 Fundamentals of Wireless Networking

In order to understand the operation of a wireless LAN, it is necessary to first examine the operation of a conventional wired LAN. LANs are used to link computers and peripherals together so that they can transfer data between them. This allows all of the computers on the network to share printers or file servers for example. A conducting medium, typically coaxial cable or twisted pair wiring is used to connect the devices on the network. On more complicated networks such as the one at the University of Tennessee, a multi-tasking mainframe computer is often connected to the network to provide e-mail and Internet services.

A wireless network performs the same functions as a wired network, but radio frequency energy is used instead of a metallic conducting medium in order to establish a link between computers and peripherals. This makes wireless network components more complicated since a carrier signal must be modulated by the data before it can be sent to the receiving terminal in order for the data to propagate through free space. This is in contrast to many wired networks where the data is sent unaltered (baseband) over the network.

2.2 Current Status of Wireless Networking Possibilities

There are several possible ways in which a wireless LAN can be implemented, the simplest of which involves only two computers and is known as a point-to-point link. In a point-to-point link, the two terminals are connected together via wireless LAN cards so that they may transmit data between themselves. This type of setup would typically be used in a home or office environment where a user wished to share data between a desktop computer and a laptop computer. It is also possible to construct an entire LAN using nothing but wireless networking hardware installed on each device. This type of architecture is known as a stand-alone wireless LAN. Currently however, the type of architecture shown in Figure 2.1 is the most common type of wireless LAN implementation [2]. In this system, a wireless access point is connected to a wired LAN so that computers that have wireless client cards installed can communicate with the rest of the wired network. This type of configuration is more common since it provides mobile users the advantage of moving freely while providing stationary clients the advantages of a wired LAN such as a higher data rate (typically five times faster than wireless LANs), lower bit error rate, and lower latency.

Most RF wireless LANs that are currently available utilize one of two modulation techniques: direct sequence spread-spectrum (DS/SS) or frequency hopping spread spectrum (FH/SS). Figure 2.2 shows the effects of spread spectrum modulation on the power spectrum of a signal. Before spread spectrum modulation, the power spectrum $G(f)$

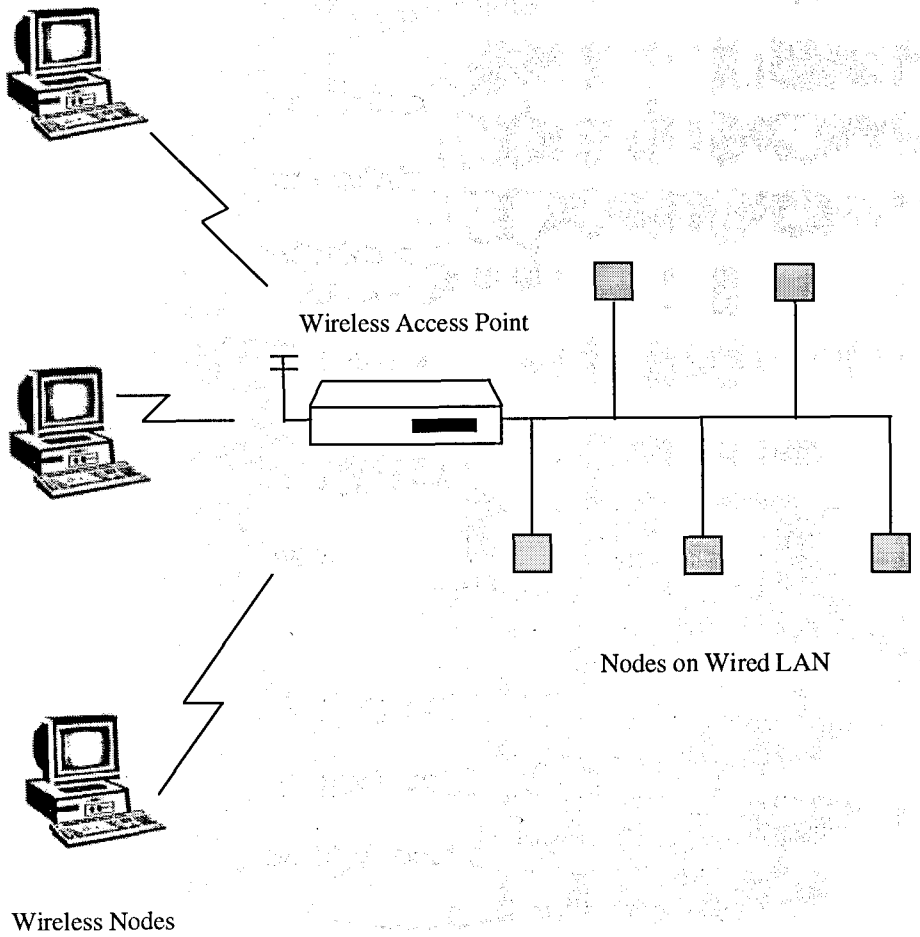


Figure 2.1 Hybrid wireless/wired LAN

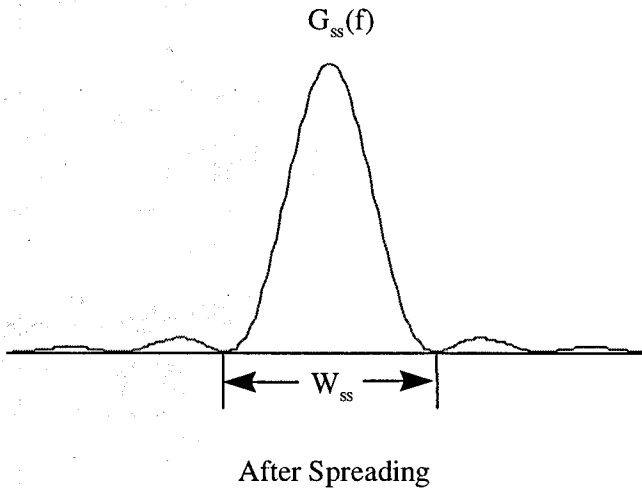
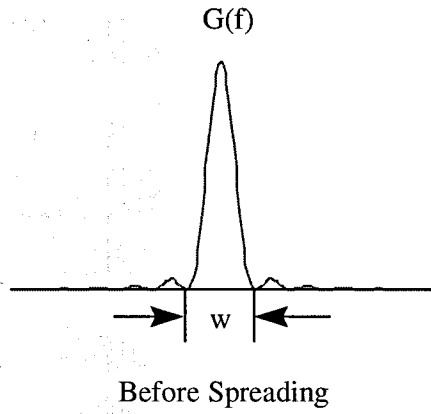
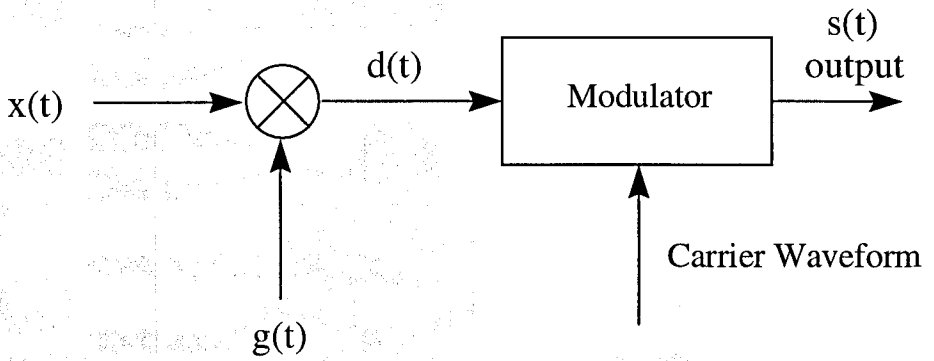


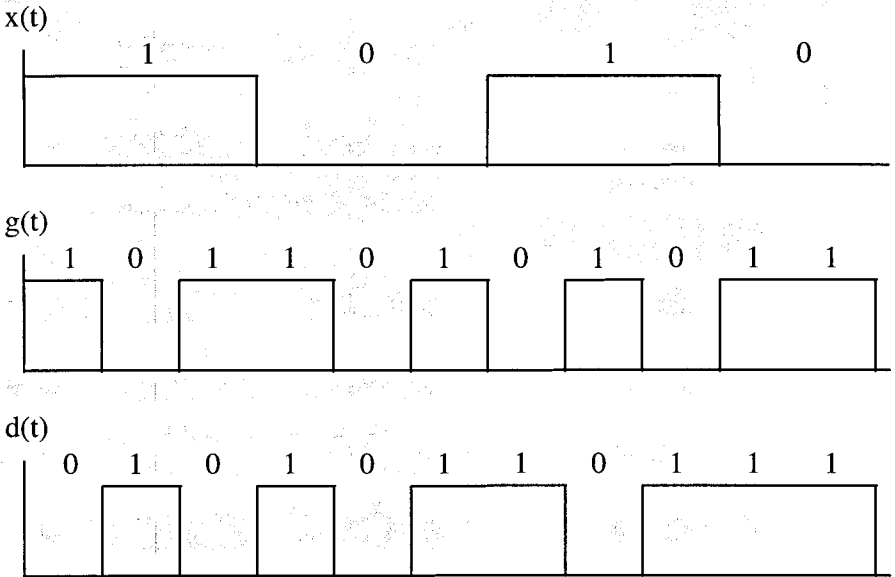
Figure 2.2 Power spectral density (a) before
(b) after spread spectrum modulation

has a bandwidth W that is much smaller than the bandwidth W_{ss} , the spectrum of the spread spectrum signal. A DS/SS system spreads the bandwidth by increasing the overall data rate of the transmission by combining the modulating data signal with a faster pseudonoise sequence. Thus the modulated carrier has a bandwidth that is dictated by the rate of the pseudonoise sequence rather than that of the data. The receiver, knowing the pattern of the pseudonoise sequence, correlates the demodulated received signal with the pseudonoise sequence to recover the data waveform. Figure 2.3a is a block diagram of a DS/SS transmitter. The data waveform $x(t)$ is combined with the pseudonoise sequence $g(t)$ using modulo-2 arithmetic. The modulo-2 sum is then used to modulate a carrier (carrier modulation is discussed in Chapter 4) in order to produce the output $s(t)$. Figure 2.3b shows typical DS/SS waveforms.

An FH/SS system operates by hopping among frequencies within the desired spread spectrum bandwidth. For a given hop, the bandwidth is the same as the original bandwidth of the data signal; however, averaged over many hops the entire spread spectrum bandwidth will be occupied [4]. A pseudonoise sequence is used to determine the order of hopping frequencies. Figure 2.4 is a block diagram of an FH/SS transmitter. The data waveform $x(t)$ modulates a carrier to produce the signal $y(t)$ which has a bandwidth W (see Figure 2.2). The FH modulator is then used to shift the center frequency of W among various frequencies within W_{ss} . Thus FH/SS can be thought of as a two step process: data modulation and frequency hopping modulation, although it is possible to accomplish FH modulation in a single step by using a frequency synthesizer that produces a carrier that is



a) DS/SS transmitter



b) DS/SS waveforms

Figure 2.3 DS/SS transmitter and waveforms

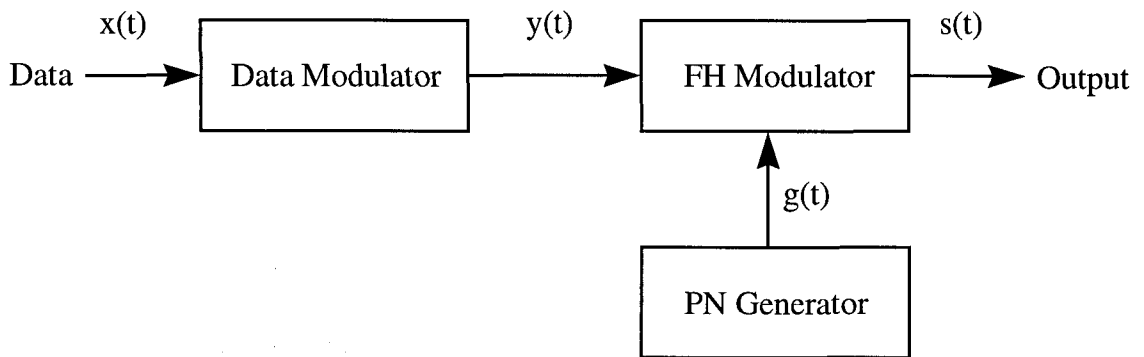


Figure 2.4 FH/SS modulator

determined by the simultaneous use of the data waveform and the output of the pseudonoise generator [4].

The pseudonoise sequence used in DS/SS and FH/SS systems is a deterministic signal that has the properties of a random signal. There are three properties that a signal must have in order to appear random [4]. The *balance property* requires that the difference in binary ones and zeroes in the sequence differ by at most one digit. The *run property* requires that the bits alternate between 0 and 1 every bit period about half the time, alternate between 0 and 1 every other bit period about one-fourth the time, alternate between 0 and 1 every fourth bit period about one-eighth the time, and so on. The *correlation property* requires that if the sequence is shifted by any cyclic period that the number of agreements (bits that are the same in the shifted sequence as the non-shifted sequence) differ from the amount

of disagreements (bits that are different in the shifted sequence from the non-shifted sequence) by not more than one. Pseudonoise sequences are used because they make it difficult for an unauthorized listener to decode the sequence since they appear random.

DS/SS and FH/SS systems both have advantages and disadvantages. FH/SS systems can be implemented with bandwidths twice that of DS/SS systems [4], yielding a greater processing gain which is a measure of the systems resistance to interfering signals. In fact, some wireless LAN vendors claim that FH/SS provides 100,000 times more immunity to interference than DS/SS [5]. However, since a DS/SS system occupies a constant bandwidth, the transmitting nodes do not need to listen to each other during lapses of data transmissions in order to maintain frequency synchronization. This is important in the case of wireless LANs where a laptop computer with a limited power resource is often used.

Both DS/SS and FH/SS systems however, have the property of minimizing multipath interference. Multipath interference is caused by reflections of the transmitted signal reaching the receiver at different times, thus distorting the received waveform. In DS/SS systems multipath interference is reduced because correlation is used in the demodulation stage. Since the chip period (a chip is one bit of the pseudonoise sequence) is shorter than the period of the data, many more of the multipath signals will arrive during a different chip period than they would a data period. Also, since the pseudonoise sequence has a small correlation between shifts, the multipath signals that arrive during a different chip period have little effect on the demodulated signal. In FH/SS systems, multipath

interference is reduced because by the time many of the multipath signals arrive, the receiver will already be tuned to another center frequency.

The reason for using spread spectrum modulation in a wireless LAN environment is because without it, the frequency bands used for wireless LAN applications have propagation characteristics that will support data rates of only 300 kbits/s [3]. However due to the multipath interference reduction in spread spectrum systems, data rates up to 2 Mbits/s can be supported within an 11 MHz spread spectrum bandwidth [3]. In 1985, the U.S. Federal Communications Commission (FCC) allocated the Industrial, Scientific, and Medical (ISM) bands for wireless LAN use [2,3]. The ISM bands are comprised of: 902-928 MHz, 2.400-2.4835 GHz, and 5.7250-5.825 GHz. Most early wireless LAN devices operated in the 902-928 MHz band due to lower implementation costs, but the current trend is toward the 2.400-2.4835 GHz band as it is the only band for which wireless LAN standards are currently under development. Some wireless vendors are developing full duplex wireless LANs that use both the 2.400-2.4385 GHz and 5.7250-5.825 GHz bands, although these systems are not yet widely available.

A third type of transmission system currently used for wireless LANs uses infrared (IR) light rather than RF energy to communicate between devices. The disadvantages of an IR system are that distances are more limited than RF systems, and there must be a line of sight between communicating devices. Thus transmission is impossible through walls and doors. Also, a wide coverage IR wireless LAN can be almost twice as expensive as one

based on RF [6]. Some of the advantages of an IR system compared to RF systems are increased security since the IR light will not penetrate walls or floors and thus the risk of eavesdropping is reduced, FCC licensing is not required for such a system, and the system is immune to RF interference. Also, IR systems have data rates comparable to wired LANs since more bandwidth is available for IR systems.

2.3 The Wireless LAN Project at Carnegie Mellon University

In March 1994 the Information Networking Institute (INI) at Carnegie Mellon University submitted a proposal to the National Science Foundation to create a “High Speed Wireless Infrastructure” [7]. In November 1994, the INI group at CMU solicited wireless LAN products for testing and received them from AT&T (Lucent division), Proxim, and Xircom. The evaluation of the wireless LAN products focused on five items [7]:

1. coverage;
2. throughput;
3. form factor;
4. ease of use; and
5. Apple Macintosh support.

It was INI's strategy not only to base their selection of a vendor upon this performance criteria, but also upon partnership arrangements that were proposed by each of the vendors. The partnership evaluation focused on three items [7]:

1. resources, expertise, and commitment;
2. ensuring the continued currency of the network; and
3. a special relationship to jointly pursue research and development.

After technical and partnership issues were evaluated, the INI group made its final selection in March 1995. The AT&T product was chosen over the other two. The AT&T product (which is now sold under the name Lucent Technologies, a subsidiary of AT&T) uses the 902-928 MHz band, DS/SS modulation, and has a nominal throughput of 2 Mbits/s. The in-building coverage was specified as 125 feet (38.1 meters) with an outdoor range of 400 feet (121.9 meters). The AT&T product also provides support for the Apple Macintosh through a third party vendor (Digital Ocean), a feature not available for the Proxim or Xircom products. At this time, the AT&T product is the only wireless LAN for which Macintosh support is available.

The INI group at CMU began a pilot installation in March 1994 to test the operation and coverage of the AT&T product and to validate the assumptions made concerning coverage area. The building selected was Wean Hall, a reinforced concrete structure with cinder block walls. Reportedly, penetration between floors was higher than had been

assumed and coverage was significantly better than the worst case scenario used in estimating access point placement [7]. Following the success of this initial test program, by September 1995 CMU had installed a total of 108 access points in five separate buildings and one outdoor area. Few difficulties were encountered in the process, the exception being lower field strength than expected in some areas.

2.4 Standards Efforts

In order for computers to exchange information, they must share a common protocol or be able to translate their respective protocols. The *IBM Dictionary of Computing* defines a protocol as: "A set of semantic and syntactic rules that determines the behavior of functional units in achieving communication." In other words, the form (syntax) and meaning (semantics) between computers on a LAN are defined by a set of rules [5]. The International Standards Organization (ISO) developed the Open Systems Interconnect Model (OSI Model) to bring a level of standardization to protocols. The OSI model (Figure 2.5) was developed to illustrate the separable functions necessary for data communications between computers. The functions of the seven layers of the OSI model as applied to LANs are as follows [8]:

Application Layer - Provides end-user services. An example would be an e-mail program such as Eudora. It is this layer with which the end user interacts.

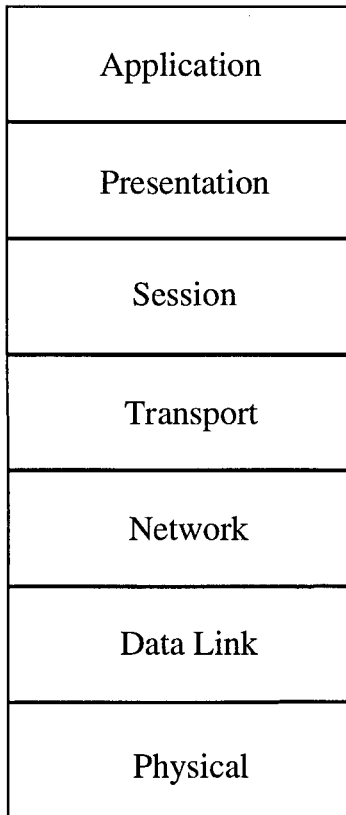


Figure 2.5 The OSI model

Presentation Layer - Responsible for the syntax (or form) in which data is exchanged between two hosts. Data encryption and data compression are examples of Presentation Layer functions.

Session Layer - Provides a logical connection between two terminals. Controls the starting, stopping, and synchronization of the data transfer.

Transport Layer - The last layer that is concerned with end-to-end communications. Error recovery and the rate of data flow are examples of transport layer functions.

Network Layer - Establishes the path from the source terminal to the destination node. Switching and routing are functions of the network layer.

Data Link Layer - Responsible for providing reliable communication between terminals. Provides a mechanism to address and transmit (both source and destination) each data packet. Also provides error control such as Cyclic Redundancy Check (CRC) for the data within each packet.

Physical Layer - Concerned with the interface to the transmission media, encoding of the data signal, voltage magnitudes, connector sizes, and generally anything to do with the physical transmission of the bit stream.

Thus, information that is generated by the user at the Application Level is modified as it moves down through the layers until it reaches the physical layer, at which point it is simply a series of bits that contain all of the information needed for reconstruction at the receiving end. The OSI model is useful for understanding how a protocol works, but most actual protocols use a different number of layers and have a different view of the function at each layer.

Two popular protocols that currently enjoy widespread use in wired LANs are the IEEE 802.3 standard and Ethernet. Both protocols address LAN standards at the Physical and Data Link layers of the OSI model. In the IEEE 802.3 and Ethernet protocols, the Data Link and Physical Layers are sub-divided into three layers; the Logical Link Control (LLC) Layer, the Medium Access Control (MAC) Layer, and a slightly redefined Physical Layer. The LLC Layer is responsible for establishing, maintaining, and terminating the logical link between computers and peripherals. The MAC layer controls access to the shared transmission medium. The Physical Layer is again concerned with the nature of the physical transmission medium.

In 1990 the IEEE formed the P802.11 Group to develop standards for wireless communications, including wireless LANs. In November 1993, the first portion of a wireless LAN standard was approved. Although the 802.11 wireless LAN standard is still being modified, the foundation of a standard does exist. The protocol addresses issues at the MAC layer and the Physical Layer. The MAC protocol for wireless LANs uses Carrier

Sense Multiple Access with Collision Avoidance (CSMA/CA) [2]. CSMA/CA attempts to avoid collisions between users that share the same bandwidth by waiting for silence on the network before a transmission is attempted. After a transmission is complete, the transmitting node waits to receive an acknowledgment of its transmission from the recipient node. If no acknowledgment is received, the transmitting node assumes a collision has occurred with another transmitting node and waits for a random period of time (in order to prevent another collision) and then re-transmits its data. The CSMA/CA scheme is similar to the CSMA/CD (Carrier Sense Multiple Access with Collision Detection) used by 802.3 and Ethernet except that with CSMA/CD, the transmitting station continues to listen to the network while transmitting so that a collision may be detected before the entire data packet is sent. Thus CSMA/CD is somewhat faster than CSMA/CA, but since nodes on a wireless LAN may not be able to hear every other node as it would on a wired LAN, the CSMA/CA scheme is better suited for wireless LANs [2]. At the Physical layer, the IEEE 802.11 standard is being developed for infrared wireless LANs, 2.4 GHz FH/SS wireless LANs, and 2.4 GHz DS/SS wireless LANs.

2.5 Product Offerings

The wireless LAN industry has seen considerable growth over the past few years and there are a number of companies that now manufacture wireless LAN products. The companies range from established, diversified corporations such as AT&T and IBM to newcomers such as AIRONET and Digital Ocean which manufacture wireless LAN products

exclusively. Table 2.1 summarizes the wireless LAN access points available from the various vendors. Included in the table are the product names, the maximum data transfer rate, frequency band used, and price as of February 1997. All of the products listed support Ethernet. Although this table almost certainly does not include all products available from all vendors, it includes the products available from manufacturers that are most actively marketing their products through magazine advertisements and World Wide Web pages. Table 2.2 summarizes the PC cards currently available from the vendors listed in Table 1. Also included is the Digital Ocean product for the Macintosh laptop that works with the Lucent access point.

Tables 2.1 and 2.2 show that there are considerable differences between performance and cost among wireless LAN vendors. In Chapter 3, these differences are discussed and a product selection for the wireless LAN at the University of Tennessee is made.

Table 2.1 Summary of wireless LAN access points

Company	Product	Speed	Frequency	Cost
AIRONET	ARLAN 630-900	860 Kbps	902-928 MHz	\$1,995
	ARLAN 630-2400	2 Mbps	2.4-2.4835 GHz	\$1,995
AT&T (Lucent)	WavePOINT	2 Mbps	902-928 MHz and 2.4-2.4835 GHz	\$1,195
Firlan	EH360	10 Mbps	Infrared	\$4,995
IBM	Model 13H5895	350 Kbps	2.4-2.4835 GHz	\$750
Proxim	RangeLAN2/7500	1.6Mbps	2.4-2.4835 GHz	\$1,490
Xircom	Netwave	1 Mbps	2.4-2.4835 GHz	\$1,499

Table 2.2 Summary of wireless LAN client cards

Company	Product	Speed	Adapter type	Price
Aironet	ARLAN 690-900	860 Kbps	PCMCIA	\$745
	ARLAN 690-2400	2 Mbps	PCMCIA	\$745
AT&T (Lucent)	WaveLAN	2 Mbps	PCMCIA	\$695
Digital Ocean	Manta 500	2 Mbps	AAUI	\$995
Firlan	ET340	10 Mbps	Connect to Ethernet 10Base2, 10Base5, or 10BaseT	\$695
IBM	Model 92G7787	350 Kbps	PCMCIA	\$230
Proxim	RangeLan2/7200	1.6 Mbps	PCMCIA	\$522
Xircom	Netwave	1 Mbps	PCMCIA	\$399

Chapter 3

A Model for Wireless Networking

3.1 Site Selection

There are several instances where a wireless LAN is more convenient or economical than a wired LAN. Although many modern buildings are constructed with wiring ducts in order to make it easy to install cable, many older buildings were constructed before the need for wiring LANs was envisioned. If the building has historical significance, it may be a very undesirable option to drill holes in order to run cables from room to room. It can also be very expensive to perform construction on such a building in order to achieve results that are aesthetically acceptable. A wireless LAN however, can be used in such a building without the need for extensive alteration.

There is also the case where hazardous materials are involved. In buildings constructed during the period when asbestos was commonly used for insulation, installing wires in the ceiling or walls can create a health hazard [2]. Also, in sealed “clean rooms” that are used for research or some production processes, it may be extremely difficult to install coax without dust or other contaminants entering the environment. In both cases however, there may often be a need to connect computers to a LAN. The use of a wireless LAN can provide this service without disturbing materials used in the construction of a building and without introducing foreign materials into a sealed environment.

In some instances, there may be only a short term need for a LAN at a particular location. A good example of this are the locations used for registration and drop-add at a university. Typically these events last only for a few weeks out of the year, but access to a LAN is required in order for the data to be stored in the University's main computers. A wireless LAN could be set up and dismantled quickly and also allow for an expanded number of terminals to be set up if required. Also, locations could be selected that are more convenient than those which already have conventional wired LAN ports installed.

Perhaps the best case for wireless LANs can be made when mobility is the key to the application [2]. With the advent of laptop computers which require no external connections, having a means by which they can access a LAN allows the user to access data from other computers, access the Internet, send e-mail, and enable printing to a printer connected to the LAN. Productivity is enhanced since the user is not required to return to a computer with a hard-wired LAN connection to perform such tasks.

At the University of Tennessee, mobility was the primary factor in deciding to implement a wireless LAN. As a pilot program, it was decided upon conferencing with the Network Services Department to install a wireless LAN in the second floor study area of Hodges Library. By placing the wireless LAN in the library, any student or faculty member who owns a laptop computer with the proper hardware installed will be able to access the University's network system. Through its network, the University of Tennessee provides services such as e-mail, Internet access, and also access to many client/server based

programs which are more time-efficient when executed on a powerful multi-tasking computer.

3.2 Proposal of an Architecture

After evaluating performance specifications of several wireless LAN vendors, the Lucent Technologies WavePOINT access point and WaveLAN PCMCIA wireless LAN adapter were chosen for the UTK wireless LAN. Of the wireless LAN products investigated, the Lucent product has an equal or greater throughput, and is the only one for which Apple Macintosh support is currently available. A meeting held in August, 1996 between University of Tennessee staff and representatives of Lucent Technologies made it clear that technical support for the Lucent product is excellent.

Lucent produces two versions of their wireless LAN system, one which operates in the 900 MHz band and one that uses the 2.4 GHz band. The 2.4 GHz version was chosen because the IEEE 802.11 standard is being developed for the 2.4 GHz band and Lucent plans to make the current product compatible with the 802.11 standard once it has been ratified.

The WaveLAN system uses direct sequence spread spectrum (DS/SS) modulation which was discussed in Chapter 2 [9]. Differential quaternary phase shift keying (DQPSK) is used to produce the transmitted carrier. Since DQPSK yields 2 bits/symbol, a symbol rate

of 1 Msymbol/s will yield a data rate of 2 Mbits/s. The phasor diagram of a DQPSK system is shown in Figure 3.1. The four quadrants represent the four possible orthogonal phase changes of the carrier signal. The system uses an 11-chip Barker sequence spreading code which increases the 2 MHz symbol rate bandwidth to an overall transmitted bandwidth of 22 MHz. This process is illustrated in Figure 3.2.

The WaveLAN system provides seamless roaming access support to mobile stations that have roaming software drivers installed. Thus a wireless station that moves from the coverage area of one WavePOINT to another (provided the coverage areas overlap) will connect to the other access point if the signal quality of the transmission is better. The quality of the signal is determined by signals that are continuously sent out by the WavePOINT and monitored by the mobile station which will start searching for another WavePOINT if the signal quality drops below a preset value. If the mobile station detects a WavePOINT station whose signal quality exceeds the preset value, the handoff occurs automatically without any interruption in service to the mobile user [10].

An important concern of wireless LAN users is the security of the data transmitted. The WaveLAN system provides four layers of security as illustrated in Figure 3.3. The first layer of protection is spread spectrum technology which was discussed in Chapter 2. Physical access to the WaveLAN signal does not yield intelligible results unless the receiver knows the pseudo-random sequence that is used to spread the bandwidth of the signal for transmission. The second layer is provided by the network identification code

2 Mbit/s \longrightarrow 1 Msymbol/s

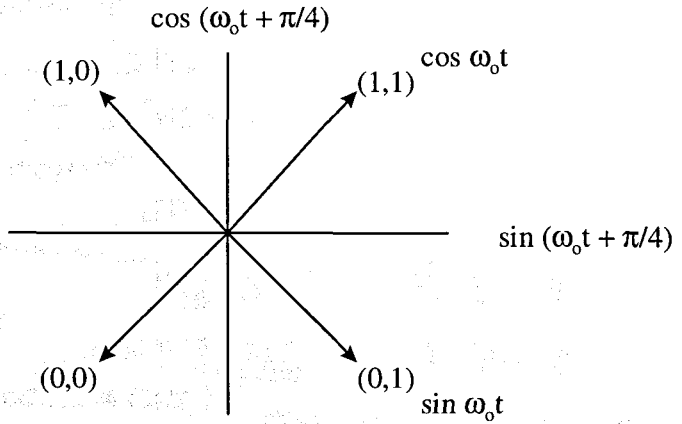


Figure 3.1 Signal space for DQPSK

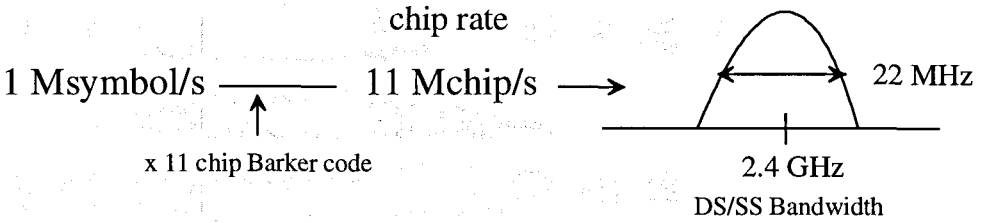


Figure 3.2 Modulation technique for DS/SS

Security Layer 1 - Spread Spectrum Technology
Security Layer 2 - 4 Digit RF-frame code (NWID)
Security Layer 3 - optional encryption
Security Layer 4 - password of LAN

Figure 3.3 WaveLAN Security Layers

(NWID). The NWID is included in each transmitted frame and communication can only take place between a mobile user and a WavePOINT access point if both are using the same NWID. The third layer of protection is data encryption. The WaveLAN system uses the data encryption standard (DES) as defined by the National Bureau of Standards. DES is a publicly known cryptographic algorithm that scrambles the data and the 64 bit encryption code (or key) so that every bit of the transmitted encrypted data depends on both the original data and the encryption key [12]. Thus in order for the data to be retrieved, the receiver must also know the encryption key. The fourth layer of protection is the user name and password required to access the LAN. This is a standard feature of the network operating system and applies to wired as well as wireless LANs [11].

3.3 The WavePOINT Access Point

The WavePOINT access point functions as the link between an Ethernet backbone and a PC laptop equipped with a WaveLAN PCMCIA card. The WavePOINT can be connected to the wired network using either a thin Ethernet with a BNC connector, thick Ethernet with an AUI connector, or an unshielded twisted pair (UTP) with an RJ45 connector [10]. The 2.4 GHz version has an output power specification of 32 mW through an omnidirectional antenna which is supplied with the unit. The approximate range of the WavePOINT is 120-180 meters in an open environment (where there are no obstructions between the antennas), 30-60 meters in a semi-open environment (such as an office area with shoulder height partitions), and 15-30 meters in a closed environment (such as an office building with walls from floor to ceiling.)

After connecting the WavePOINT to the wired LAN, it must be configured using software that is shipped with the unit. Installing this software is a 3-step procedure [10]. First, a "Configurator" workstation must be selected. This can be a workstation that is connected to the wired LAN or it can be a wireless station. Second, a utilities diskette is created using the software included with the WavePOINT. This utilities diskette contains programs such as the PtPMeasure utility which will be thoroughly examined in Chapter 5. Third, a configurator environment diskette is created again using the software included with the WavePOINT.

The configurator diskette is used to set the parameters of the WavePOINT. The unit is shipped with default parameters already loaded so that it may be used right out of the box. The first parameter that may be changed from its default is the network ID (NWID), a four digit hexadecimal number which the wireless stations must also be set to in order to communicate with the WavePOINT (the default value is the last four digits of the WavePOINTs serial number.) The encryption key can also be changed using the configurator diskette. For units operating in the 2.4 GHz band, there are several sub-bands which may be selected as the operating frequency and this can also be changed by the configurator software.

In addition to these basic parameters, there are more advanced parameters that can be changed to fine tune the performance of the WavePOINT. It is possible to prevent transmissions from a particular station on the wired LAN from being broadcast to the wireless stations by specifying its MAC address. It is also possible to specify the MAC addresses of wireless stations that are authorized to access the WavePOINT in a table to prevent unauthorized users from accessing the network. Finally, it is possible to adjust the sensitivity thresholds that define when a wireless station will begin searching and hand over to another WavePOINT when roaming.

Once the desired configuration has been saved to the configurator diskette, the serial number of the WavePOINT that is being configured is simply entered into the program,

and the configuration information is passed on to the WavePOINT. The WavePOINT will then function as defined by the configuration data.

3.4 The WaveLAN PCMCIA Card

The WaveLAN PCMCIA card is a device that connects to the PCMCIA socket of a portable computer allowing it to communicate with a WavePOINT access point. Included with the WaveLAN PCMCIA card is an antenna module and software drivers needed to configure the card for correct operation. The 2.4 GHz version transmits 50 mW of power and has a specified range of 180-240 meters in an open environment, 48-60 meters in a semi-open environment, and 27-33 meters in a closed environment.

The WaveLAN drivers have been developed to take advantage of PCMCIA Card and Socket Services [13]. If Card and Socket Services are installed on the computer then the WaveLAN PCMCIA card can be installed quickly using the *INSTALL.EXE* program that is included with the card. The *INSTALL.EXE* program will install the WaveLAN drivers, support and utility files, and will update system files to include the correct initialization parameters.

The WaveLAN PCMCIA card provides a power management feature which allows the card to be put in a low-power consuming state when no active communication is taking place. The card becomes active at regular intervals in order to remain connected to the

network since some networks will disconnect a user after a period of inactivity. While in the low-power mode, the card uses only 0.175 Watts compared to 1.575 Watts in the receiving mode and 1.825 Watts while in the transmit mode. Thus in the low-power mode, the unit uses only about 15 percent of the power used in the receive mode which can significantly improve the battery life in mobile workstations [13].

The software shipped with the WaveLAN PCMCIA card includes the Point-to-Point Diagnostic Utility (PtPMeasure) which allows the user to make measurements of the communications quality between the laptop PC and the WavePOINT access point. The PtPMeasure utility allows the user to make measurements about the signal level, signal-to-noise ratio, and the percentage of packets successfully received. The PtPMeasure utility is used to evaluate the performance of the system in this thesis and is discussed in Chapter 5.

Chapter 4

Simulation

4.1 Introduction

In this chapter, a direct sequence spread spectrum (DS/SS) DQPSK transmitter and receiver similar to that used by the WaveLAN system is simulated. A multipath channel is also modeled in order to make the simulation as realistic as possible. The simulation is created using LabVIEW, a graphical programming language produced by National Instruments [21]. First an overview of the DS/SS DQPSK system and its error performance is given followed by a description of an indoor multipath channel. Finally the simulation is described and its performance evaluated.

A LabVIEW program involves two parts; the front panel and the block diagram. The block diagram contains specialized virtual instruments (VIs) which perform functions on data such as computing a Fast Fourier Transform (FFT) or producing a sinusoidal pattern. Simpler functions such as addition and multiplication are also accomplished in the block diagram. The front panel is a graphical user interface that contains controls and graphs that are used to change the input data and view the output data, respectively.

4.2 Transmitter/Receiver Characteristics

4.2.1 DQPSK Modulation

The WaveLAN System uses Differential Quaternary Phase Shift Keying (DQPSK). DQPSK is used because it eliminates the need for the receiver to be absolutely synchronized to the carrier phase of the transmitted signal. In a DQPSK receiver the phase of the current symbol is compared to the phase of the preceding symbol in order to make a decision. This type of demodulation is referred to as differentially coherent phase shift keying. The implementation of DQPSK presupposes two things: (1) the unknown relative phase shift of the received signal due to the channel characteristics is constant over at least two symbol periods, and (2) the phase during a given signaling interval bears a known relationship to the phase during a preceding signaling interval [14]. The first condition is determined primarily by the stability of the carrier oscillator while the second condition can be met by employing differential encoding of the data at the transmitter.

Differential encoding of the data waveform, $d(k)$, is accomplished as shown in Figure 4.1.

The encoded sequence, $c(k)$, is given by the expression:

$$c(k) = \overline{c(k-1) \oplus d(k)} \quad (4.1)$$

This EXCLUSIVE-OR operation (\oplus) on the data sequence with a delayed version of the encoded sequence ensures that a relationship exists between successive points in the

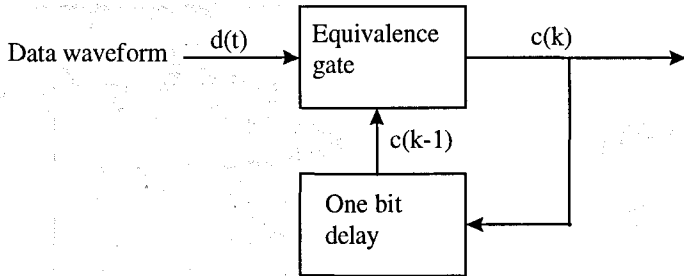


Figure 4.1 Block diagram of a differential encoder

encoded sequence, $c(k)$. The encoded sequence is then used to determine the phase of the transmitted waveform. The receiver can then recover the encoded waveform by detecting the phase change between symbol periods. The data waveform $d(k)$ can then be recovered by performing the operation:

$$d(k) = \overline{c(k) \oplus c(k-1)} \quad (4.2)$$

In the case of DQPSK, the data waveform $d(k)$ is divided into two waveforms containing alternating bits of $d(k)$. These are referred to as an in-phase waveform $d_i(k)$ and a quadrature waveform $d_q(k)$. These waveforms are encoded as described by Equation (4.1) to produce two encoded waveforms $c_i(k)$ and $c_q(k)$ which are used to modulate the DQPSK carrier. Since there are two possible values for each there is a total of four possible combinations which are used to produce a phase change between symbol periods of either 0, 90, 180, or 270 degrees.

4.2.2 Correlation Properties of a DS/SS Signal

The WaveLAN system uses direct sequence spread spectrum (DS/SS) modulation in order to reduce the effects of multipath interference which was discussed in Chapter 2. DS/SS increases the bandwidth of the transmitted signal by combining a pseudonoise sequence with the output of the DQPSK modulator thus effectively increasing the transmitted data rate. This process is illustrated in Figure 4.2. The DQPSK waveform is multiplied by the

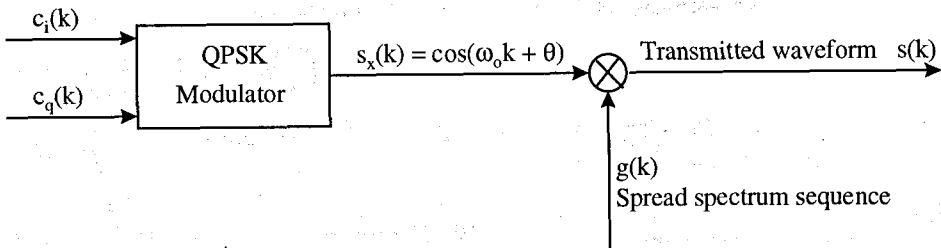


Figure 4.2 Spread spectrum modulator

pseudonoise sequence, $g(k)$, in order to produce the transmitted waveform, $s(k)$. This method differs from that shown in Figure 2.3a in that the pseudonoise sequence is multiplied with the modulated carrier rather than the data waveform. However, the two methods yield equivalent results since multiplication is commutative. The WaveLAN uses an 11-chip Barker sequence for the pseudonoise sequence. A Barker sequence is used because it has good aperiodic correlation properties, meaning that the correlator at the receiver can easily detect when it has obtained synchronization with the transmitted signal since any shift rather than a periodic shift will result in an output from the correlator that is approximately equal to zero [15]. The autocorrelation function of the Barker sequence is shown in Figure 4.3. For any shift of the sequence (other than a periodic shift) the autocorrelation function is equal to $-1/N$ where N is the number of chips in the sequence.

As previously stated, multipath interference occurs when the transmitted signal arrives at the receiver via multiple paths. The reflected and thus delayed signals interfere with the direct path signal at the receiver. This is illustrated in Figure 4.4. The signal that arrives at the transmitter can be expressed as:

$$r(t) = Ax(t)g(t) \cos(\omega_o t) + \alpha Ax(t - \tau)g(t - \tau) \cos(\omega_o t + \theta) + n(t) \quad (4.3)$$

where the first term represents the signal that arrives via the direct path, the second term represents the signal that arrives via the indirect path, α is the attenuation factor of the indirect path, τ is the delay of the indirect path relative to the direct path, and $n(t)$ is a zero

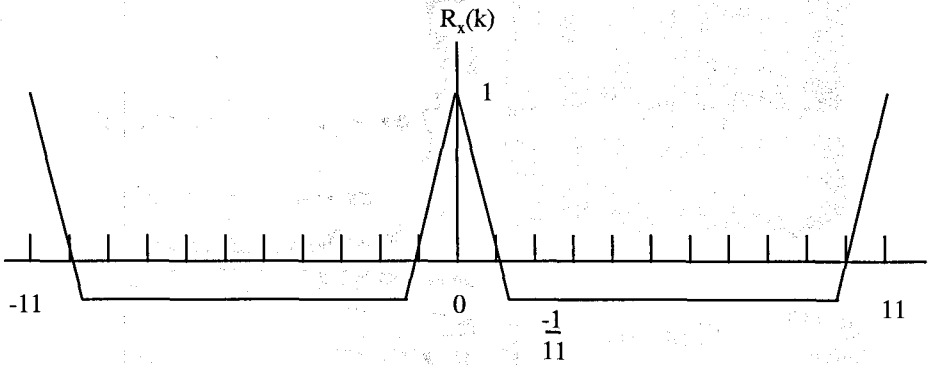


Figure 4.3 Autocorrelation function of an 11-chip Barker sequence

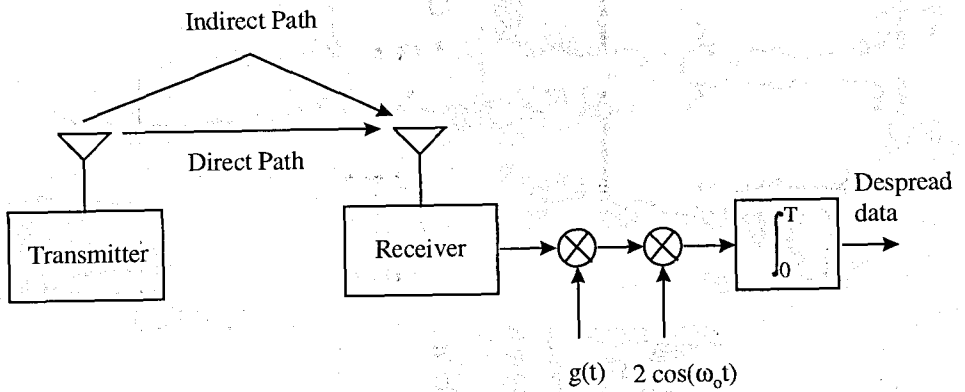


Figure 4.4 Spread Spectrum demodulator

mean Gaussian noise process. The angle θ is a random phase uniformly distributed between 0 and 2π . If the receiver is synchronized to the direct path signal, the output of the correlator, $z(t = T)$, can be written as:

$$z(t = T) = \int_0^T [Ax(t)g^2(t) \cos(\omega_o t) + \alpha Ax(t - \tau)g(t)g(t - \tau) \cos(\omega_o t + \theta) + n(t)g(t)]2 \cos \omega_o t dt \quad (4.4)$$

since $g^2(t) = 1$ and $g(t)g(t - \tau) \cong 0$ when $\tau > T_c$ where T_c is the chip period of the PN sequence, Equation (4.4) can be written:

$$\begin{aligned} z(t = T) &= \int_0^T 2Ax(t) \cos^2(\omega_o t) + 2n(t)g(t) \cos(\omega_o t) dt \\ &= Ax(T) + n_o(T) \end{aligned} \quad (4.5)$$

Where $n_o(T)$ is a zero mean Gaussian random variable. Thus it can be seen from (4.5) that the multipath signals which are delayed by more than a chip period are essentially eliminated [4].

4.2.3 Error Performance of a DQPSK System

A block diagram of a DQPSK receiver is shown in Figure 4.5. The phase of each symbol is computed by the dual correlators and then delayed by one symbol period. The phase of

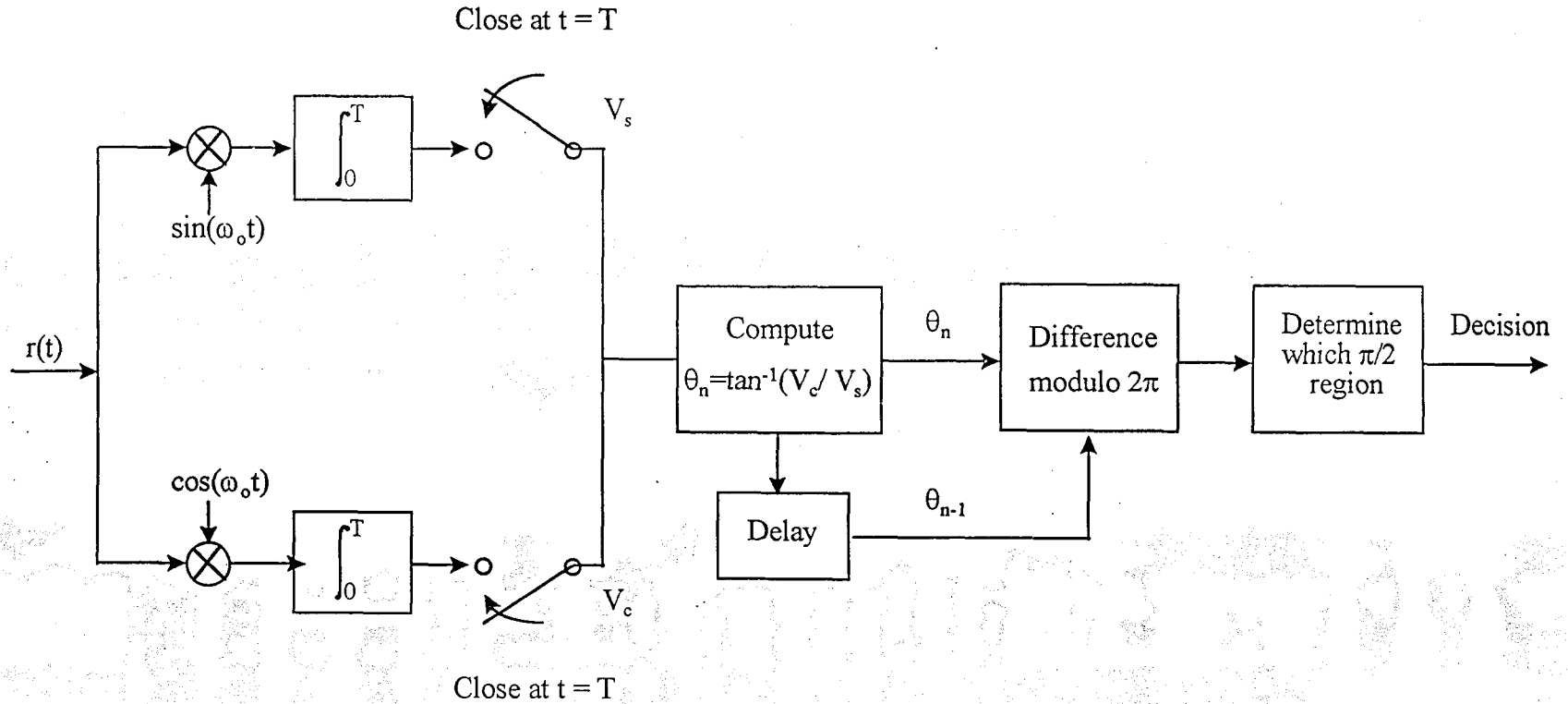


Figure 4.5 Block diagram of a DQPSK receiver

the previous symbol, θ_{n-1} , is then subtracted from the phase of the current symbol, θ_n , so that the phase difference can be determined. It has been shown [14,16] that the probability of detecting an incorrect phase difference (or equivalently a symbol error) using this method is equal to:

$$P_e(s) = \frac{1}{2} \sin \frac{\pi}{4} \int_z^{\infty} \exp(-y) I_0 \left\{ y \cos \frac{\pi}{4} \right\} dy \quad (4.6)$$

Where z is the signal-to-noise ratio of the received signal and I_0 is the modified Bessel function of order zero. There is no closed form solution for Equation (4.6); however, for large signal-to-noise ratios a useful approximation for the symbol error is given by [14]:

$$P_e(s) \approx \frac{1}{2} \operatorname{erfc} \left(\sqrt{z} \sin \frac{\pi}{8} \right) \quad (4.7)$$

The WaveLAN system uses a Gray code for the bit-to-symbol assignments meaning that adjacent decision regions of the signal constellation (Figure 3.1) have a difference of only one bit. Thus in the case of a large signal-to-noise ratio, a symbol error will usually result in only one bit error. In this case, the bit error, $P_e(b)$ can be related to the symbol error, $P_e(s)$, by the expression [4]:

$$P_e(b) \approx \frac{1}{2} P_e(s) \quad (4.8)$$

The approximate probability of symbol error using Equation (4.7) is plotted in Figure 4.6. In this chapter, analysis will be done by measuring the symbol error rates rather than bit error rates since small signal-to-noise ratios will be examined for which Equation (4.8) is not valid.

4.3 Indoor Multipath Channel Characteristics

Indoor radio frequency propagation analysis is complicated due to the fact that delayed versions of the transmitted signal which are reflected from walls and objects will arrive at the receiver and interfere with the direct signal (see Figure 4.4). This type of interference is referred to as multipath fading. Statistical models have been developed which estimate both the amplitude and time delay characteristics of indoor channels. These models are based on the impulse response of the indoor channel, $h(t)$, which can be expressed as [1, 17]:

$$h(t) = \sum_k^{N-1} \alpha_k \delta(t - \tau_k) e^{j\theta_k} \quad (4.9)$$

where N is the number of multipath components, α_k is the random amplitude, τ_k is the propagation delay, δ is the dirac delta function, and θ_k is a random phase uniformly distributed in the interval $[0, 2\pi]$.

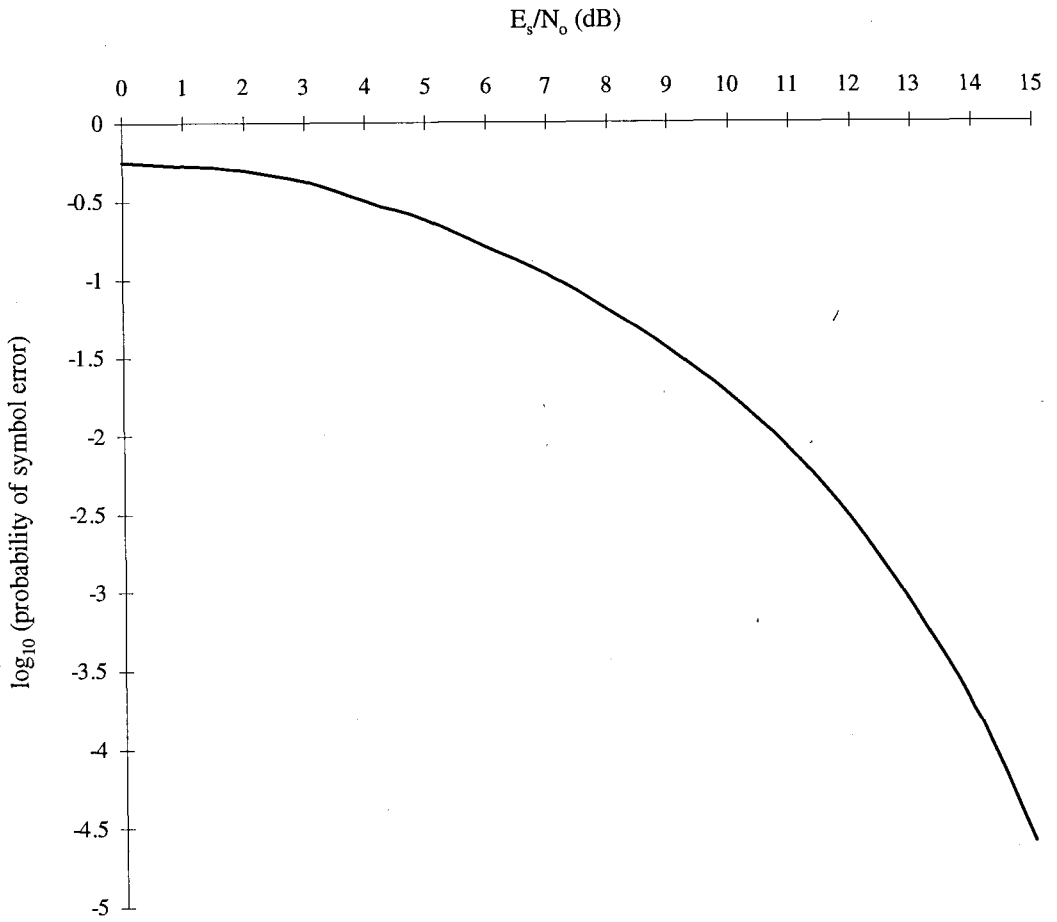


Figure 4.6 Approximate probability of symbol error for DQPSK modulation

The amplitudes of the individual path components have been successfully modeled using a Rayleigh distribution to define the strength of the multipath components relative to the direct path [17, 18, 19]. The probability density function (pdf) of a Rayleigh random variable is given by:

$$p(r) = \frac{r}{\sigma^2} \exp\left(-\frac{r^2}{2\sigma^2}\right) \quad ; \quad 0 \leq r < \infty \quad (4.10)$$

Where σ^2 is the variance of the distribution. A plot of the Rayleigh pdf with $\sigma^2=1$ is shown in Figure 4.7.

There are several parameters used to quantify the time dispersion parameters of a multipath channel. These are determined by measuring the power delay spectrum, G . The power delay spectrum is the sum of all multipath power gains and can be expressed as [1]:

$$G = \sum_k \alpha_k^2 \quad (4.11)$$

The three most commonly encountered time dispersive statistics are the mean excess delay (τ), the rms delay spread delay (σ_τ), and the maximum excess delay (τ_{max}). The maximum excess delay is simply the time at which the received power falls below a pre-defined level relative to the strongest received component. The mean excess delay is the first moment of the power delay profile and is defined as [18]:

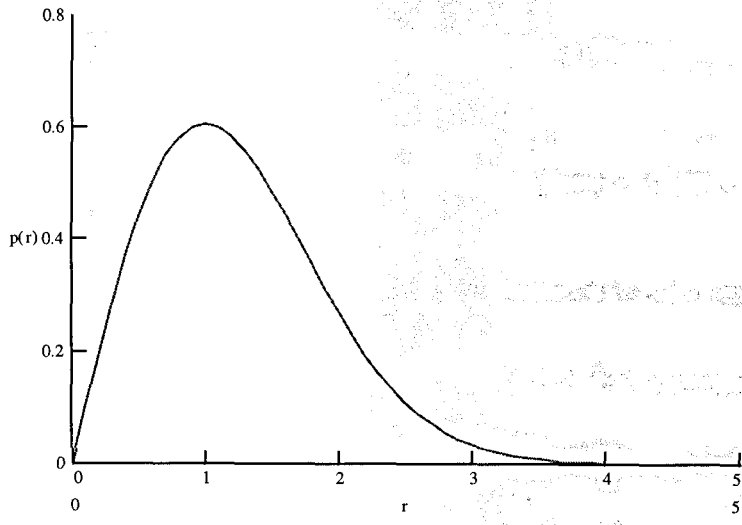


Figure 4.7 Rayleigh pdf

$$\bar{\tau} = \frac{\sum_k \alpha_k^2 \tau_k}{\sum_k \alpha_k^2} \quad (4.12)$$

The rms delay spread is the square root of the second central moment of the power delay profile and is defined as:

$$\sigma_\tau = \sqrt{\tau^2 - (\bar{\tau})^2} \quad (4.13)$$

where

$$\tau^2 = \frac{\sum_k \alpha_k^2 \tau_k^2}{\sum_k \alpha_k^2} \quad (4.14)$$

An example of an indoor power delay profile which illustrates the time dispersion parameters is shown in Figure 4.8.

4.4 System Simulation Description

In this section a description of the LabVIEW simulation used to measure bit error rates for a DS/SS DQPSK system is given. First the transmitter simulation is discussed, then the multipath channel and finally the receiver.

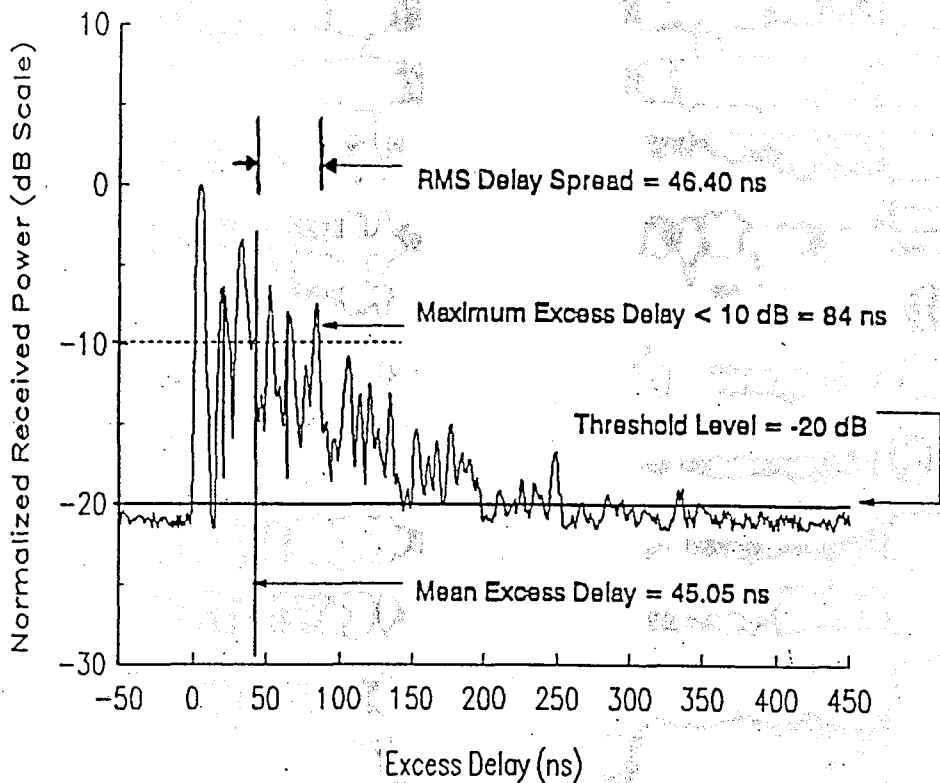


Figure 4.8 Example of an indoor power delay profile

Reprinted from: Theodore S. Rappaport, "Wireless Communications: Principles & Practice"
 © Prentice Hall, New Jersey, 1996.

4.4.1 Transmitter Simulation

A block diagram on which the DQPSK transmitter simulation is based is shown in Figure 4.9. The first stage in the transmitter simulation is to generate a random data waveform. An actual DQPSK transmitter divides the data waveform into even and odd components as discussed in Section 4.2.1. To simplify the simulation however, these two waveforms are generated independently. The LabVIEW front panel and block diagram that accomplishes this, *DAANDDQ.VI* is shown in Figure 4.10. The function of this sub-VI is to generate two random variables, d_i and d_q which can have values of +1 or -1 with equal probability. The next stage of the transmitter simulation, *STREAM.VI*, is shown in Figure 4.11. This sub-VI generates a two data streams $d_i(k)$ and $d_q(k)$ by using a *for-next* loop. The number of bits N is input on the front panel and thus the index k will range from $k = 0, 1, \dots, N/2$ so that the sum of both arrays will equal N .

The next sub-VI in the transmission process is named *ENCODE.VI* and is shown in Figure 4.12. The function of *ENCODE.VI* is to differentially encode the data waveforms as defined by Equation 4.1. Shift registers are used so that the values of $c_i(k)$ and $c_q(k)$ from the previous iteration of the *for-next* loop are available for the computation of $c_i(k)$ and $c_q(k)$ during the current iteration.

The final sub-VI in the transmitter simulation is named *GENDQPSK.VI* shown in Figure 4.13. The function of this sub-VI is to produce a DS/SS DQPSK waveform from the

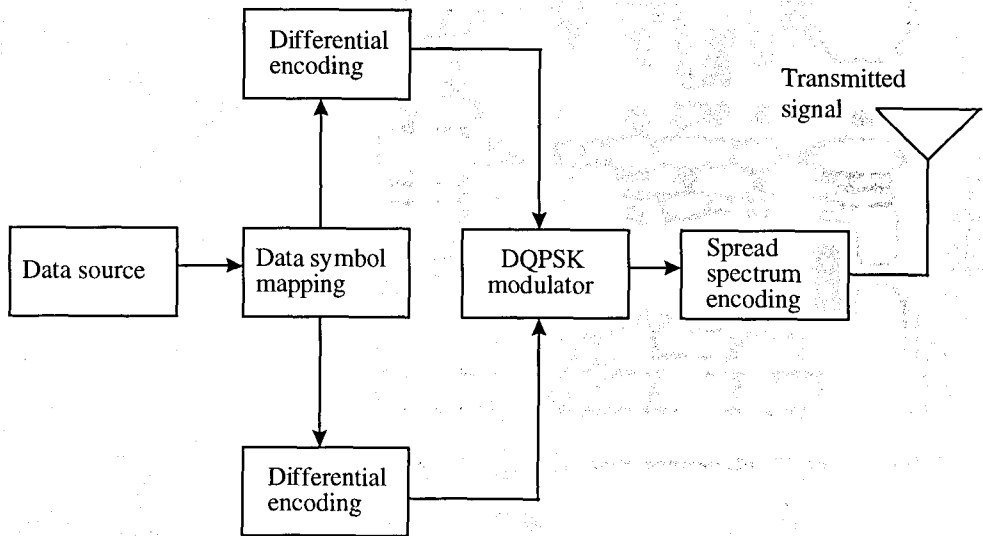
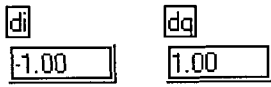


Figure 4.9 Block diagram of a spread spectrum DQPSK transmitter

Front Panel



Block Diagram

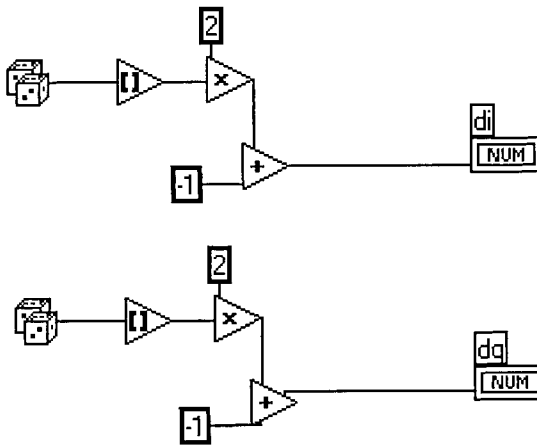
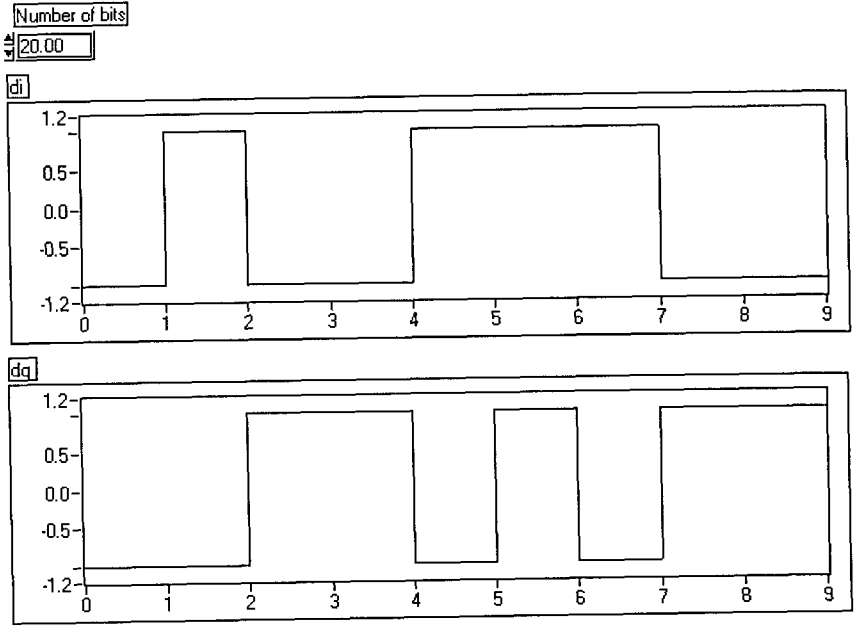


Figure 4.10 "DIANDDQ" sub-VI

Front Panel



Block Diagram

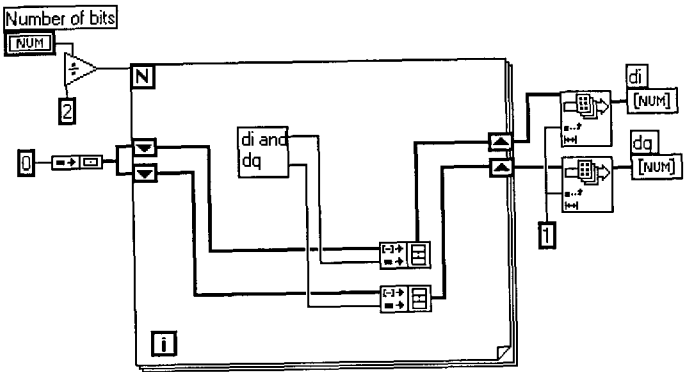
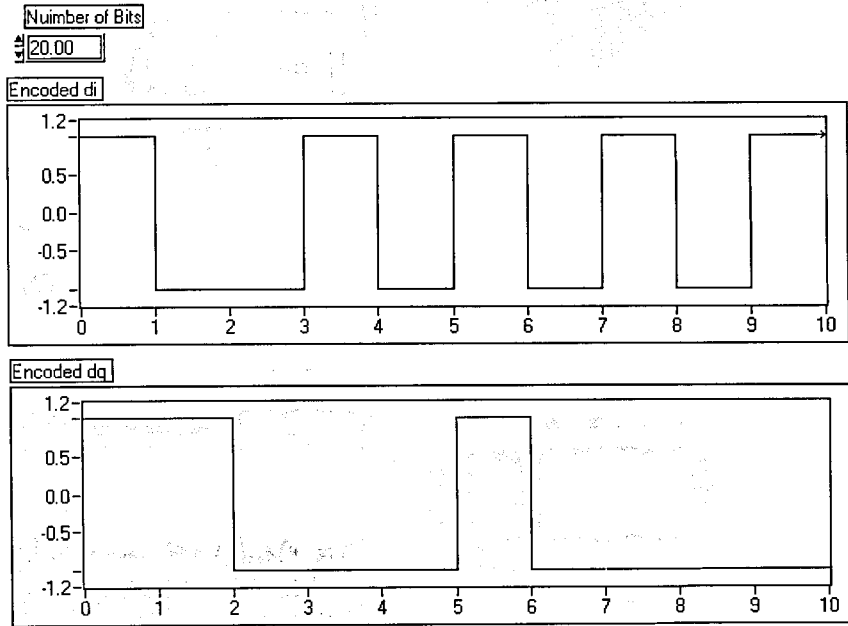


Figure 4.11 "STREAM" sub-VI

Front Panel



Block Diagram

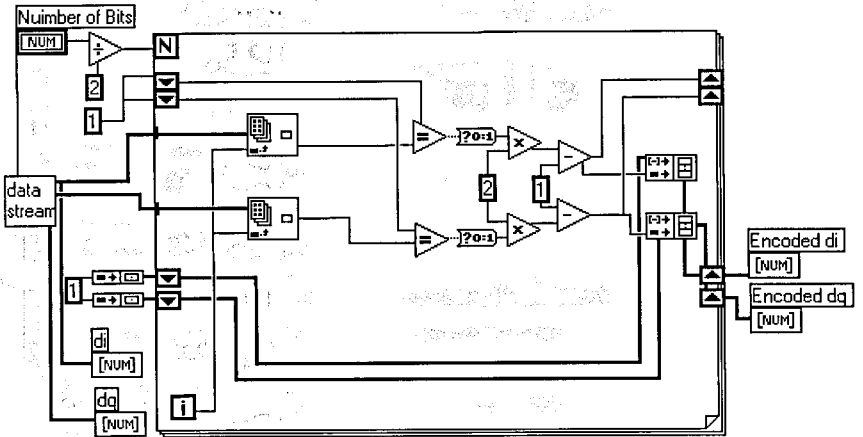
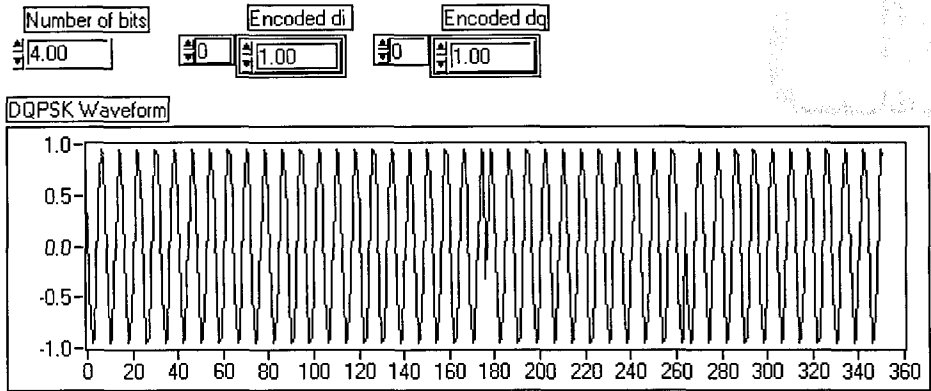


Figure 4.12 "ENCODE" sub-VI

Front Panel



Block Diagram

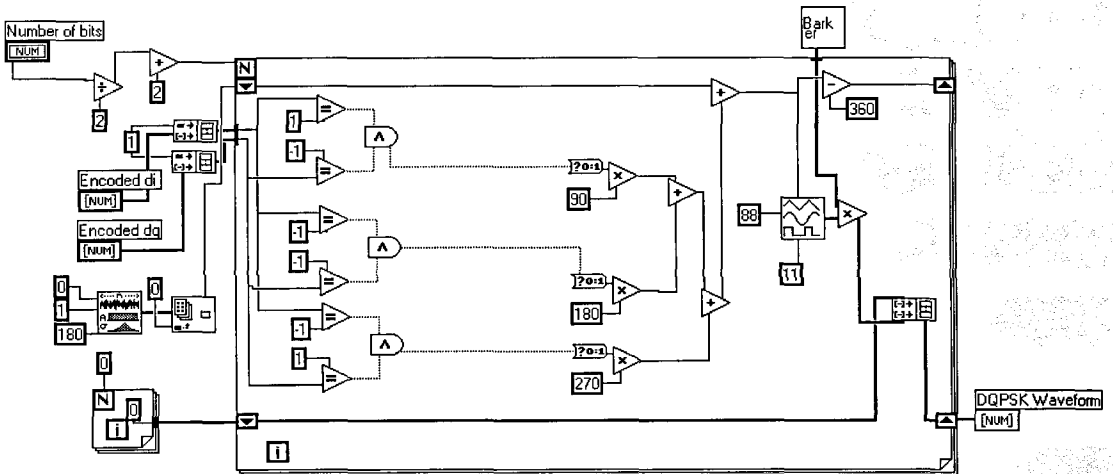


Figure 4.13 "GENDQPSK" sub-VI

differentially encoded data. The mapping of the values of $c_i(k)$ and $c_q(k)$ to the change of phase of the DQPSK waveform are as given in Table 4.1

Table 4.1 Symbol assignments

$c_i(k)$	$c_q(k)$	$\theta_n - \theta_{n-1}$ (degrees)
1	1	0
1	-1	90
-1	-1	180
-1	1	270

Although in the actual WaveLAN system there are approximately 220 cycles of the 2.4 GHz carrier waveform for each period of the 11 MHz Barker sequence, one cycle of the carrier waveform is used per chip in order to increase the speed of the simulation. Thus 11 cycles of the sinusoidal carrier waveform are produced for each bit period with 8 samples generated for each cycle. The phase of the waveform is random and uniformly distributed between 0 and 360 degrees, and the amplitude of the waveform is equal to 1. The sub-VI *BARKER.VI* is shown in Figure 4.14. A *for-next* loop is used to repeat each digit of the Barker sequence for 8 samples so that it can be multiplied by one cycle of the DQPSK waveform. Thus the output of the *GENDQPSK.VI* sub-VI is expressed as:

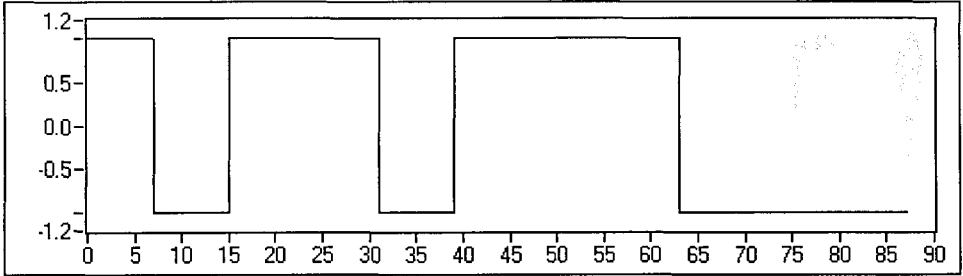
$$x(p) = g(n) \sin\left(\frac{\pi}{4} p + \theta_n + \theta_{rand}\right) \quad (4.15)$$

Front Panel

Barker on/off



Barker sequence



Block Diagram

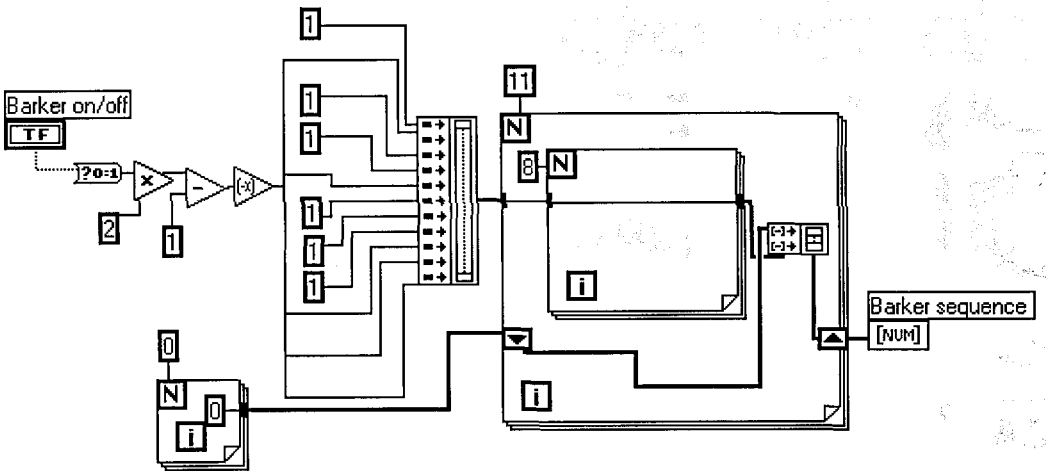


Figure 4.14 "BARKER" sub-VI

Where the p is the sample index, n is the bit index, $g(n)$ is the Barker sequence, θ_n is the phase during a given bit period (which is always a multiple of 90 degrees), and θ_{rand} is the uniformly distributed random phase.

4.4.2 Channel Simulation

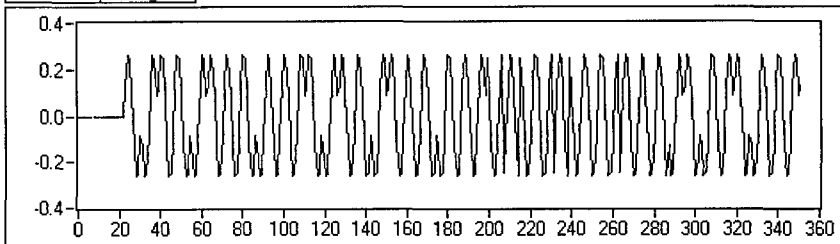
The multipath channel simulation produces delayed versions of the waveform produced by the *GENDQPSK.VI* sub-VI of the transmitter. The number of paths is specified by the user and the delay of the paths are uniformly distributed between 0 and τ_{max} . For this simulation, τ_{max} is assumed to be 600 ns which is a typical value based on the rms delay spread for an indoor environment [3, 18]. Since the chip period of the DS/SS DQPSK signal is 90.9 ns, the maximum number of samples by which the waveform will be delayed is equal to $(600 \text{ ns} / 90.9 \text{ (ns/chip)}) \times (8 \text{ (bits/chip)}) = 53$ samples.

The channel sub-vi which produces the delayed multipath signals is named *MULTPTHS.VI* and is shown in Figure 4.15. The inner *for-next* loop is the same as the *GENDQPSK.VI* sub-VI of the transmitter. It is inside another *for-next* loop that generates a number of multipath components that can be adjusted on the front panel. The time delay is created by using another *for-next* loop which outputs an array of zeroes which has a length uniformly distributed between 0 and 53 which is appended to the beginning of the DQPSK waveform. The multipath components are given amplitudes which have a Rayleigh distribution by using the sub-VI *RAYLEIGH.VI* which is shown in Figure 4.16. To

Front Panel



Sum of multipath signals



Block Diagram

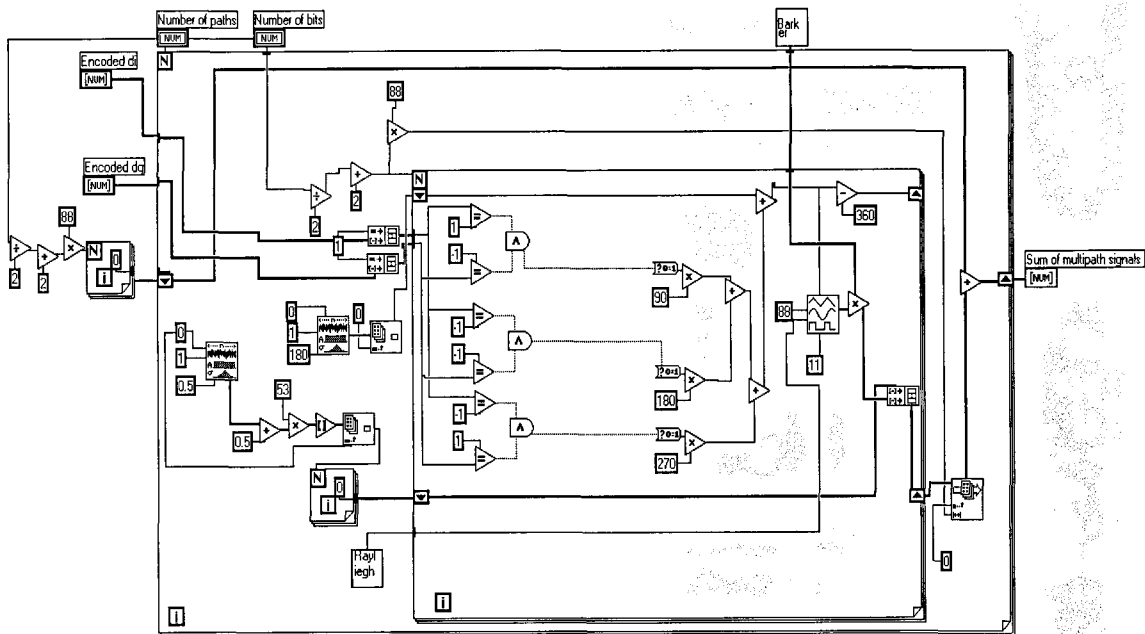


Figure 4.15 "MULTPTHS" sub-VI

Front Panel

Rayleigh Variable
0.00

Block Diagram

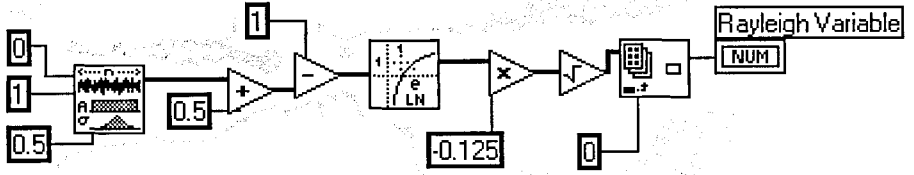


Figure 4.16 "RAYLEIGH" sub-VI

produce a Rayleigh distribution, the percentile transformation method of generating an arbitrary random distribution from a zero-to-one uniform distribution is used [1]. This transformation is expressed as [1, 20]:

$$x_i = F_x^{(-1)}(u_i) \quad (4.16)$$

where x_i has a Rayleigh distribution, u_i has a uniform distribution in the interval (0,1), and $F_x^{(-1)}(u_i)$ is a Rayleigh cumulative distribution function (CDF) with parameter u_i . The Rayleigh CDF is given by:

$$F_x(x) = 1 - e^{-x^2/2} \quad (4.17)$$

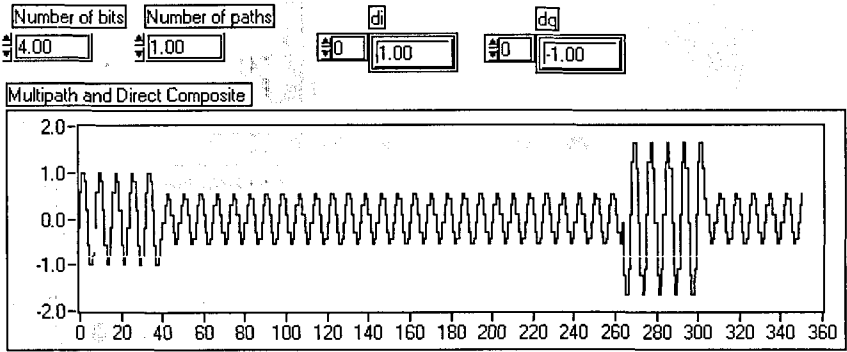
and thus the transformation takes the form:

$$F_x^{(-1)}(u) = \sqrt{-2\ln(1-u)} \quad (4.18)$$

which is the function used to produce the Rayleigh distributed random amplitudes. The multipath components are summed within the outer *for-next* loop and output to the front panel.

The sub-VI *COMPOS.VI* shown in Figure 4.17 is used to add the direct signal to the summation of the multipath components. The final VI in the channel simulation is named *CHANNEL.VI* and is shown in Figure 4.18. The purpose of this VI is to add Additive

Front Panel



Block Diagram

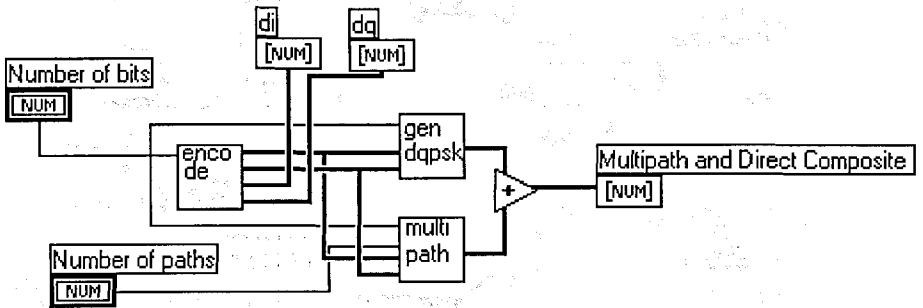
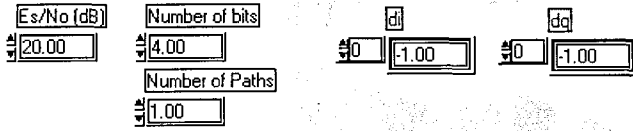
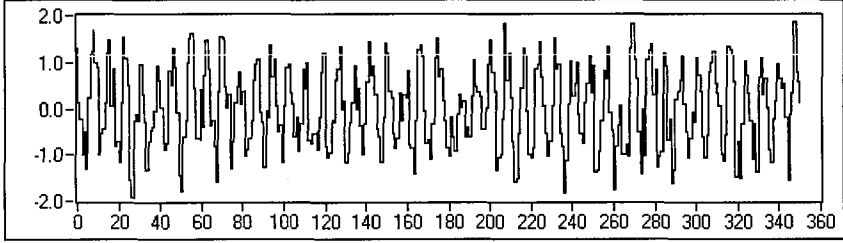


Figure 4.17 "COMPOS" sub-VI

Front Panel



Multipath signal with noise



Block Diagram

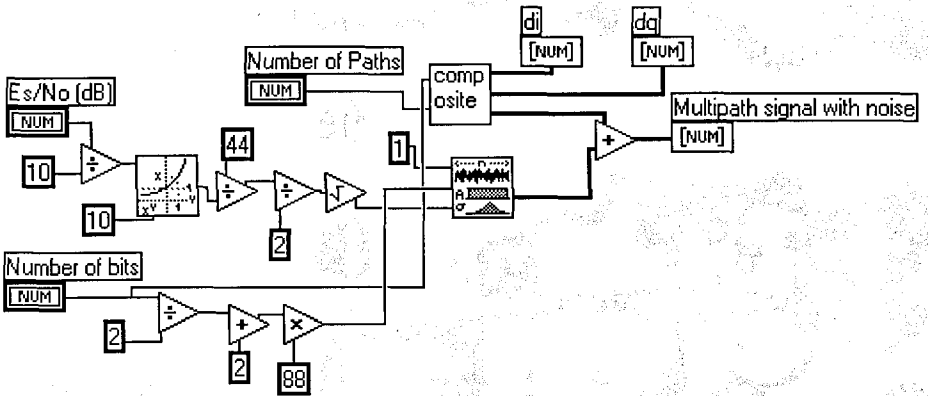


Figure 4.18 "CHANNEL" sub-VI

White Gaussian Noise(AWGN) to the signal. The desired signal-to-noise ratio (SNR) is input on the front panel. The SNR is defined as:

$$SNR = \frac{E_s}{N_0} \quad (4.19)$$

where

$$E_s = \frac{A^2 T}{2} = \frac{(1)^2 (88)}{2} = 44 \quad (4.20)$$

and

$$N_0 = 2\sigma^2 \quad (4.21)$$

where σ^2 is the variance and N_0 is the double-sided power spectral density of the AWGN.

4.4.3 Receiver Simulation

The DS/SS DQPSK receiver is based on the block diagram shown in Figure 4.19. The first receiver sub-VI, *RECEIVER.VI*, is shown in Figure 4.20. The function of this sub-VI is to first despread the DS/SS signal and then to measure the phase difference between consecutive symbol periods as illustrated in Figure 4.5 and discussed in Section 4.2.3. The sub-VI *ADDARRAY.VI* is shown in Figure 4.21. It uses a *for-next* loop to add the

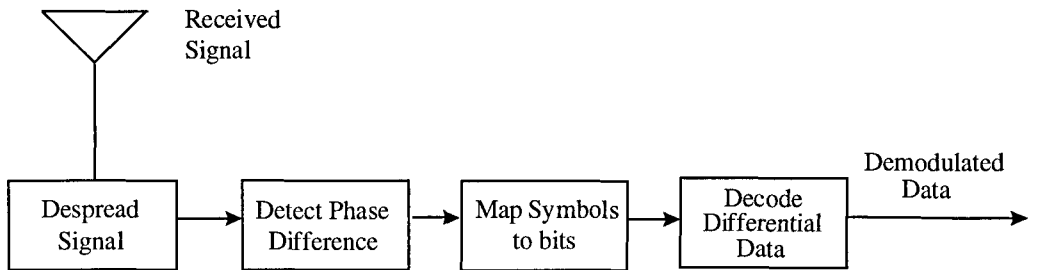
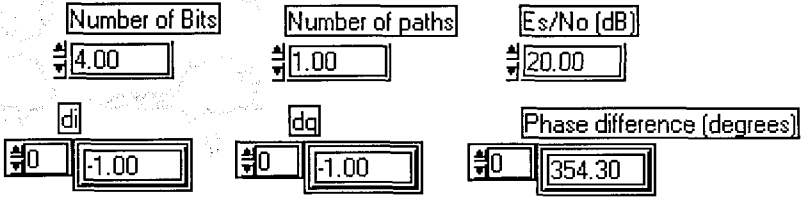


Figure 4.19 Block diagram of a spread spectrum DQPSK receiver

Front Panel



Block Diagram

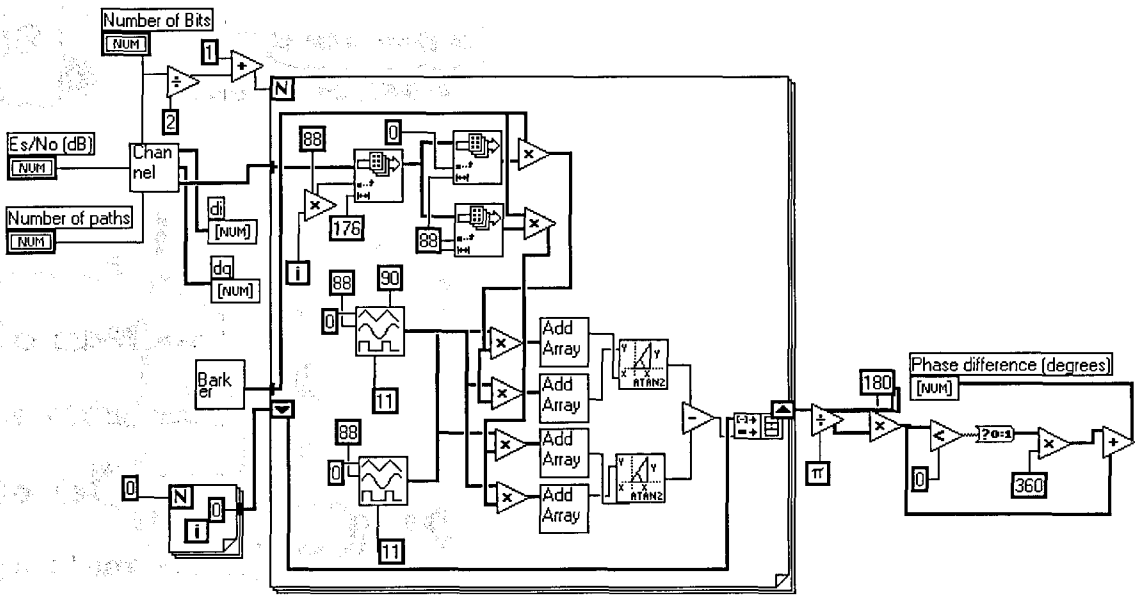
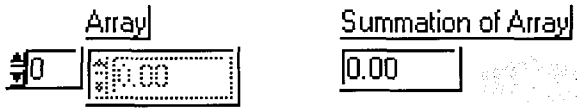


Figure 4.20 "RECEIVER" sub-VI

Front Panel



Block Diagram

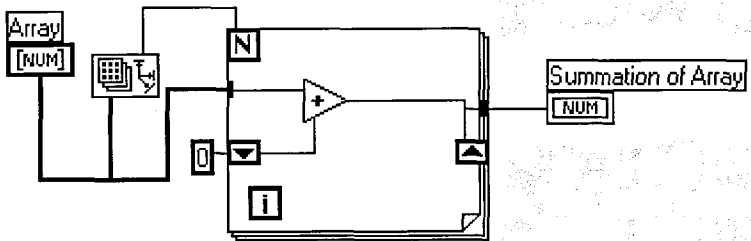


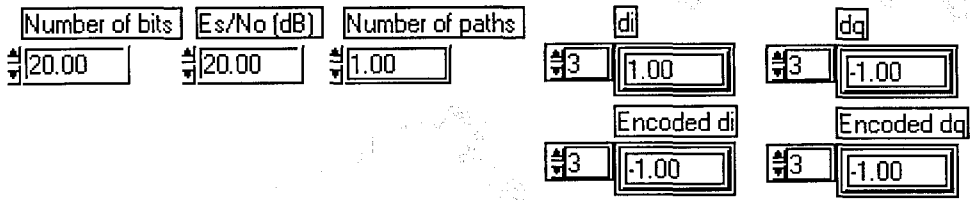
Figure 4.21 "ADDARRAY" sub-VI

elements of the input array and functions as an integrator in this VI. The phase differences are converted to degrees (modulo 360 degrees) and output to the front panel.

The next receiver sub-VI is named *DEMOD.VI* and is shown in Figure 4.22. The function of this sub-VI is to output demodulated versions of $c_i(k)$ and $c_q(k)$ based on which 90 degree decision region the output from *RECEIVER.VI* is located. The symbol to bit assignments are equivalent to those used for modulation which were shown in Table 4.1. In order to convert the encoded data waveforms $c_i(k)$ and $c_q(k)$ to the original data waveforms $d_i(k)$ and $d_q(k)$, the sub-VI *DECODE.VI* was created. It is shown in Figure 4.23. This VI compares successive values of $c_i(k)$ and $c_q(k)$ to produce $d_i(k)$ and $d_q(k)$ as given by Equation (4.2).

The final sub-VI of the receiver simulation is *BITERR.VI* and is shown in Figure 4.24. This sub-VI measures the number of bits and symbols incorrectly received by comparing the demodulated versions of $d_i(k)$ and $d_q(k)$ to the actual values of $d_i(k)$ and $d_q(k)$ that were used to modulate the carrier in the transmitter simulation. The total number of bit and symbol errors are summed using *ADDARRAY.VI* (Figure 4.21) and returned to the front panel.

Front Panel



Block Diagram

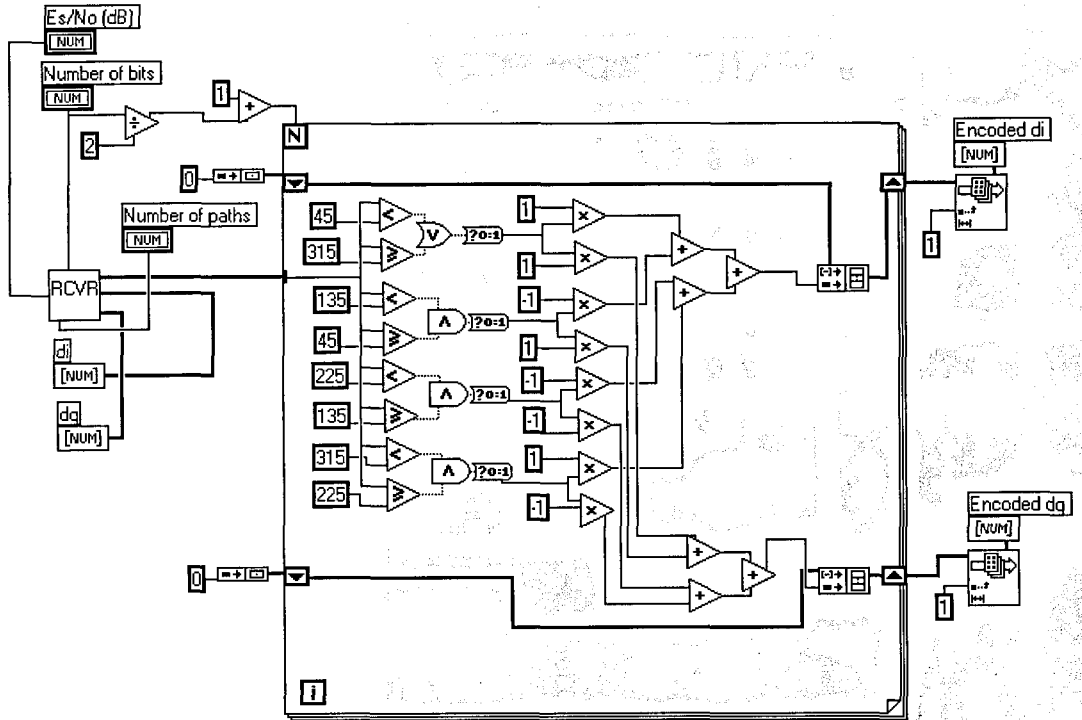
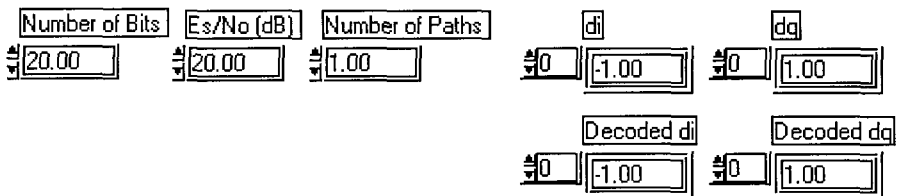


Figure 4.22 "DEMOD" sub-VI



Block Diagram

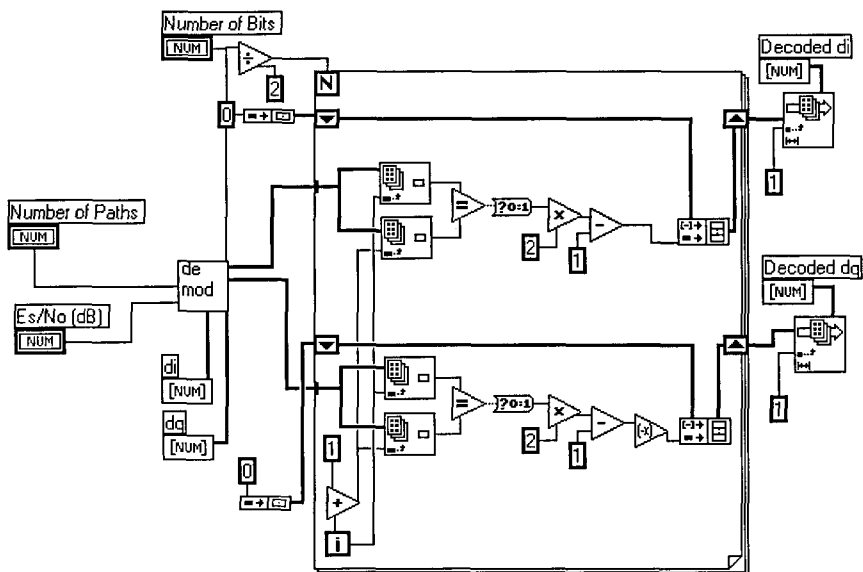
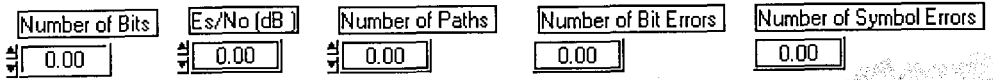


Figure 4.23 “DECODE” sub-VI

Front Panel



Block Diagram

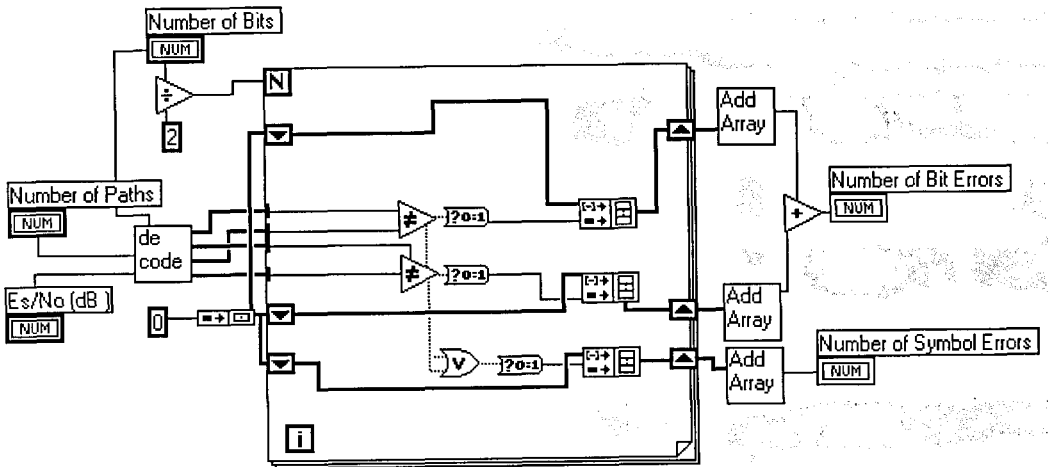


Figure 4.24 "BITERR" sub-VI

4.5 Simulation Results

In order to ensure that the simulation was operating properly, the symbol error performance was measured without multipath interference and compared to the approximate symbol error probability as given by Equation (4.7). The results are shown in Figure 4.25. The symbol error rates (SER) are within an order of magnitude throughout the range of SNR with the errors becoming smaller for increasing values of E_s/N_0 .

To measure the effects of multipath interference the simulation was run with 2, 5, and 10 paths. All measurements were done by running the simulation 10 times with the number of bits set to 1000 (500 symbols) and averaging the SERs. The results for 2 paths are shown in Figure 4.26 with the error performance for no multipath interference plotted as a reference. It can be seen that for large signal-to-noise ratios where noise is less likely to cause errors that multipath interference degrades the error performance of the system. The error performance for 5 and 10 paths is plotted in Figures 4.27 and 4.28, respectively. By comparing Figures 4.26, 4.27, and 4.28, it can be seen that increasing the number of paths increases the error rate of the system.

It should be noted that multipath signals which arrived later than the 90.9 ns chip period were observed to have negligible effects on the error performance of the system. Thus the error performance of the actual system will be highly dependent on the environment in which it is located. If there are metal objects near the transmitter or receiver that reflect

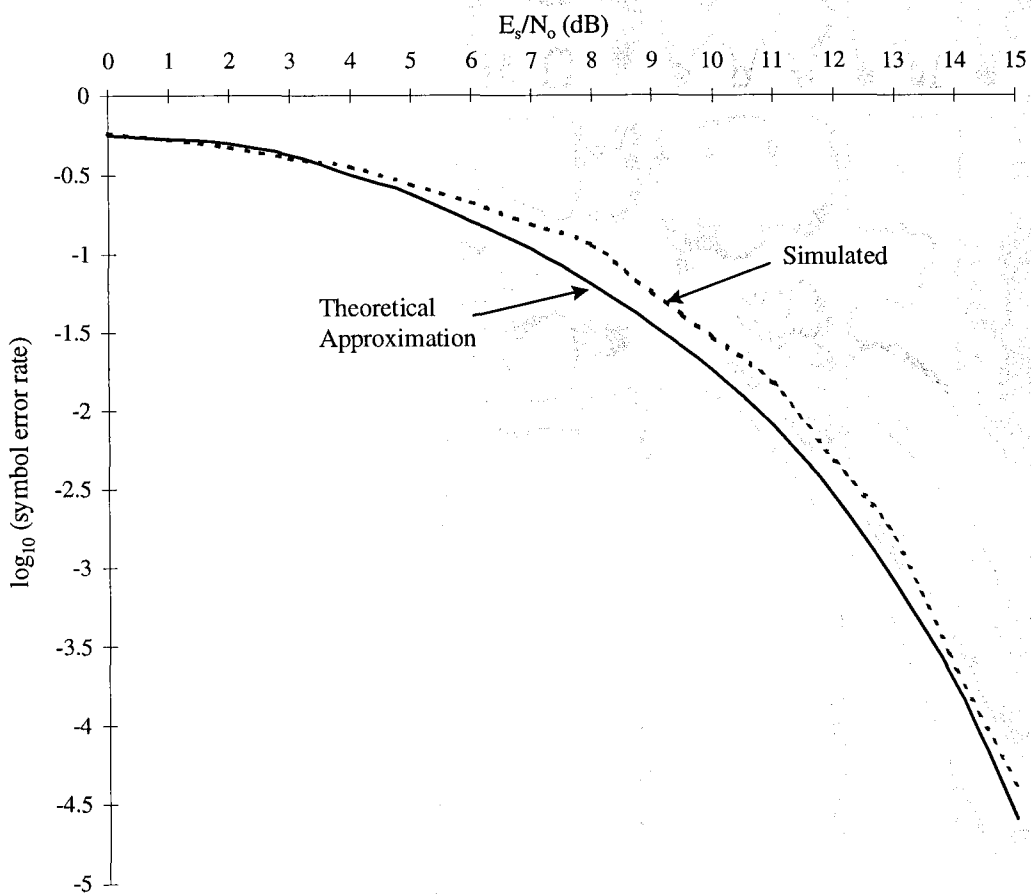


Figure 4.25 Simulated and theoretical symbol error rates (no multipath interference)

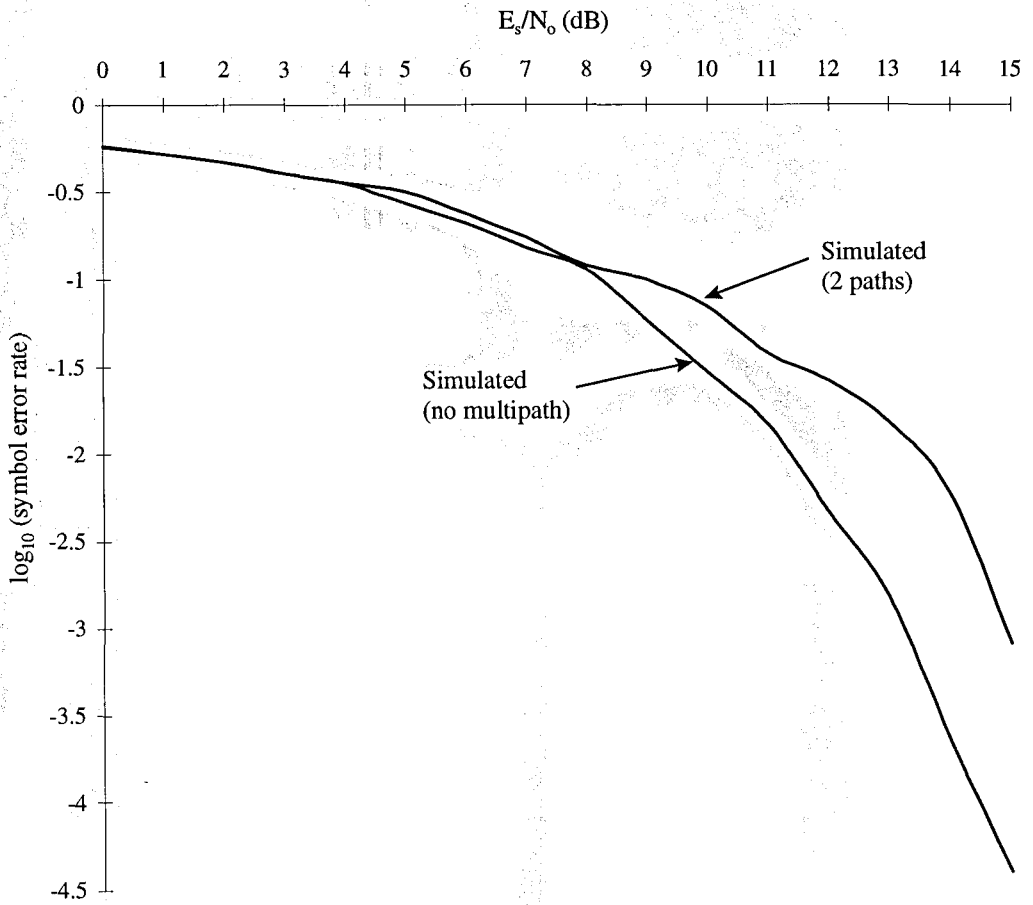


Figure 4.26 Symbol error rate with 2 paths

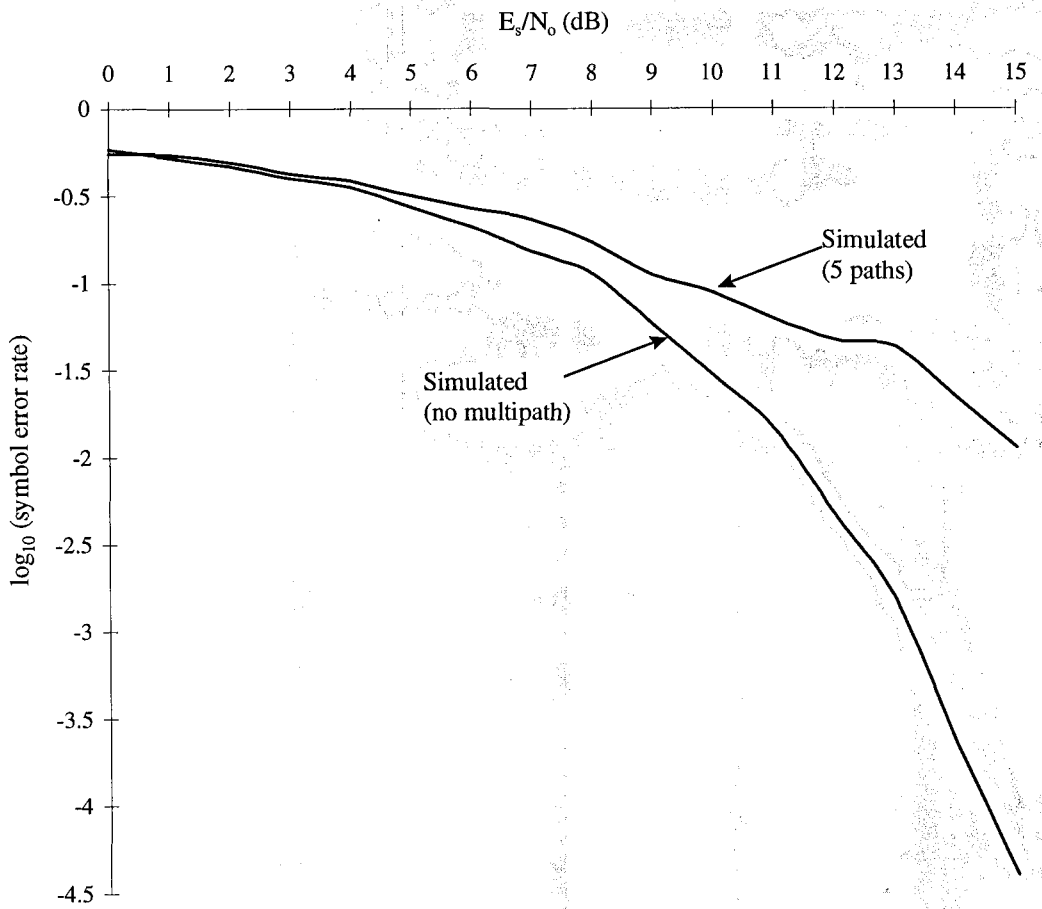


Figure 4.27 Symbol error rate with 5 paths

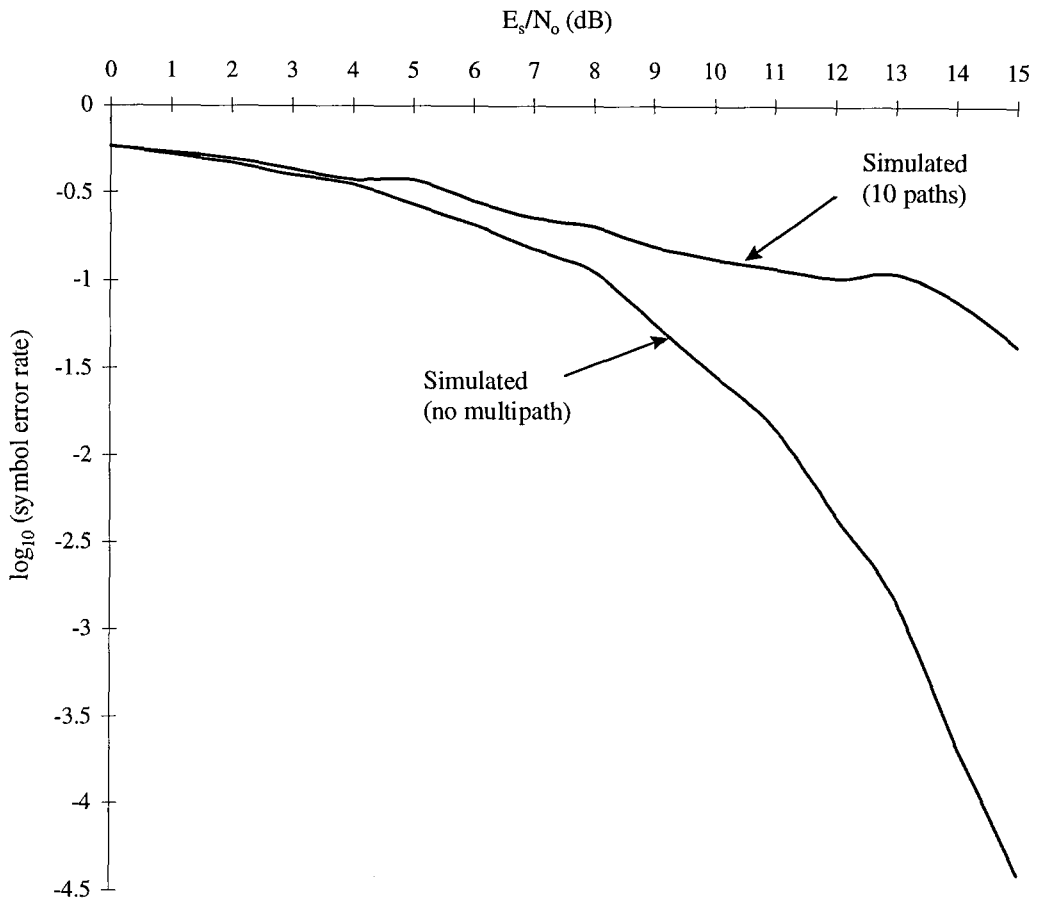


Figure 4.28 Symbol error rate with 10 paths

signals so that their delay is less than $(90.9 \text{ ns}) \times (3 \times 10^8 \text{ m/s}) = 27.3 \text{ meters}$ then appreciable multipath interference will be expected. Signals which experience a longer delay than 27.3 meters however will have little effect on the performance of the system due to the correlation properties of DS/SS. In order to illustrate the effectiveness of DS/SS against multipath interference, the simulation was run with 2 paths with and without the use of DS/SS. The results are shown in Figure 4.29. For an E_b/N_0 of 15, the average error performance is improved by a factor of 40 by using DS/SS.

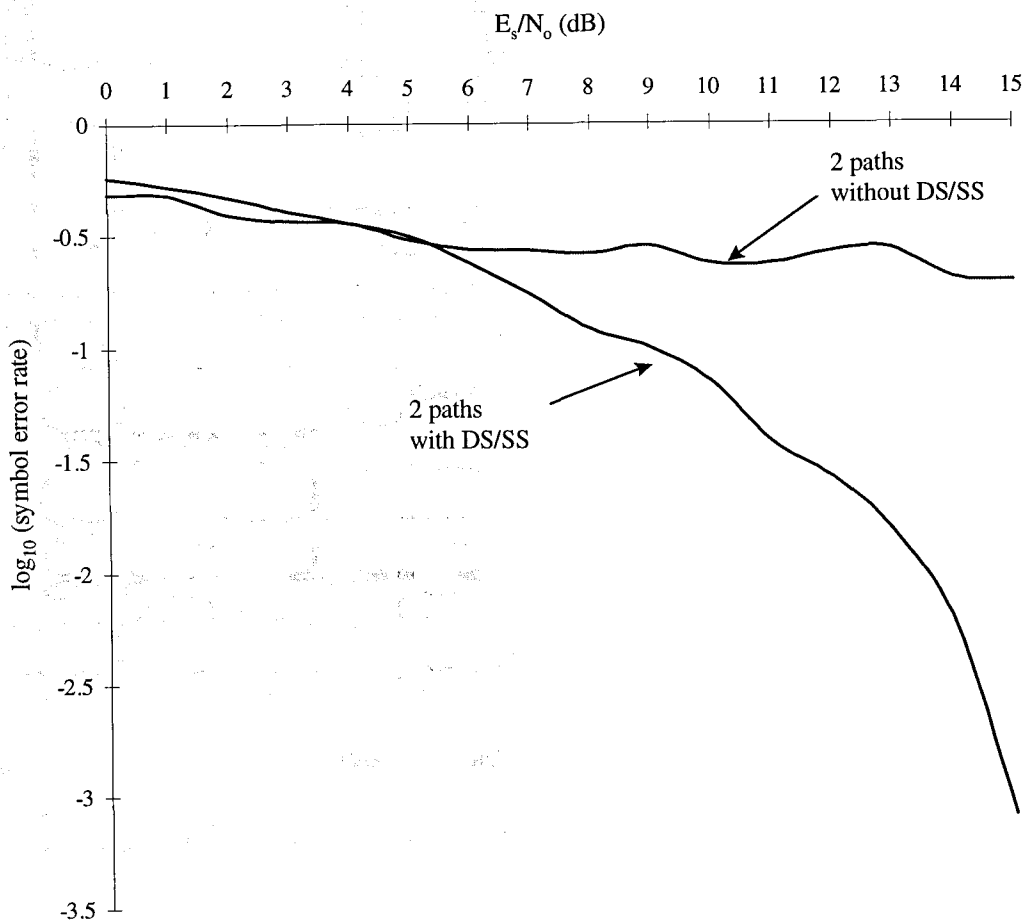


Figure 4.29 Error performance with and without DS/SS

Chapter 5

Field Tests

5.1 Introduction

In this chapter, the performance of the WaveLAN system that was installed in the second floor study area of Hodges library is evaluated. The PtPMeasure software utility which comes with the WaveLAN system was used to take measurements of the system's signal strength and signal-to-noise ratio (SNR). First a description of the PtPMeasure frame format is given, followed by a description of calculations used to evaluate the system's performance. Next a description of the environment in which the system is operating is given and finally the performance of the system is evaluated.

5.2 WaveLAN Physical Frame Format

The physical frame format used by WaveLAN is shown in Figure 5.1. It is the entire sequence of data that will be transmitted over the channel. The training pattern is the initial contact between two WaveLAN or WavePoint transceivers and is used to set timing and gain in the receiver. The length of the training pattern is 236 bytes. The start delimiter (SD) is 8 bytes long and is used by the receiver to obtain synchronization for the remainder of the frame. The carrier training sequence is 16 bytes in length and is used to determine the frequency offset between transmitter and receiver and to fine tune the

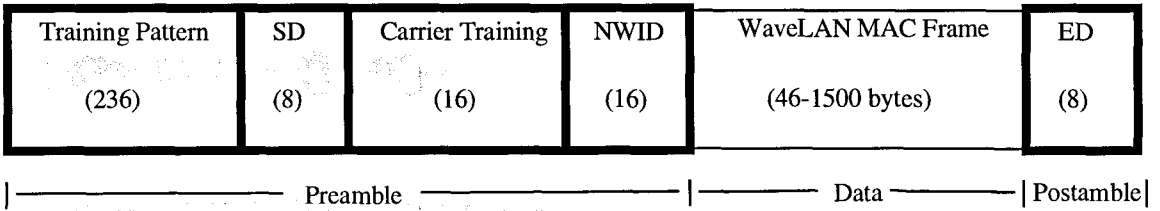


Figure 5.1 WaveLAN physical frame format

Reprinted from: Leo Monteban and Henri Moelard, "Data Manual: WaveLAN Air Interface", © 1997 AT&T

carrier frequencies so as to compensate for the offset. The NWID field contains the 16 byte network identification designator that is assigned to the station. The End Delimiter (ED) is 8 bytes in length and is used to detect the end of a transmitted frame. The Medium Access Control (MAC) layer contains between 64 and 1518 bytes and is discussed in the next section.

5.3 WaveLAN MAC Frame Format

The WaveLAN MAC frame format is the same as the IEEE 802.3 frame and is shown in Figure 5.2. The MAC preamble is 1 byte of alternating one and zero bit values which is normally used (in a wired LAN) to obtain synchronization between transmitter and receiver. However since in a WaveLAN system this is achieved by the Start Delimiter (SD) in the physical frame, it serves no purpose but is included to maintain adherence with the 802.3 protocol. The start of frame delimiter (SFD) is a one byte field with the bit sequence '10101011' that indicates the start of a frame. The destination address and source address fields are 6 bytes in length and contain the unique addresses of the transmitting and receiving stations. The length field contains 2 bytes of data that indicates the number of bits to follow in the data field. The data field is between 64 and 1500 bytes long. It contains the data generated by the higher level protocol that is to be transmitted. The frame check sequence field (FCS) contains 4 bytes that are compared to a checksum that the receiver generates via a complex polynomial. If the calculated checksum does not match the checksum on the frame, the frame is discarded.

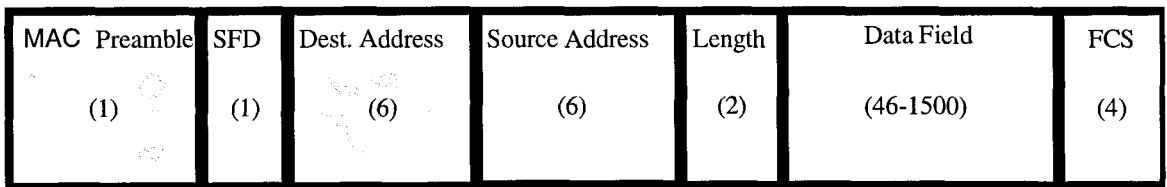


Figure 5.2 WaveLAN MAC frame format

Reprinted from: Leo Monteban and Henri Moelard, "Data Manual: WaveLAN Air Interface", © 1997 AT&T

5.4 SNAP Frame

The PtPMeasure program uses one of several special WaveLAN higher protocol frame structures that are based on a sub-network access protocol (SNAP). The SNAP concept allows for WaveLAN specific protocols as well as standard protocols to be defined. The structure of a SNAP frame and its placement in a WaveLAN MAC frame is shown in Figure 5.3. The first two frames are the destination logical link control address (also known as DSAP) and the source LLC address (also known as SSAP.) They are 1-byte in length and are equal to a hexadecimal value of AA to indicate that the message being sent is a SNAP message. The control field is one byte in length and has a hexadecimal value of 03 to indicate that it is an unnumbered information frame. The WaveLAN higher protocol identifier frame is divided into two sections; the organizationally unique identifier (OUI) which is 3 bytes long and is equal to 08-00-0E hexadecimal to indicate that it is an AT&T owned protocol and a 2-byte specific ID code that identifies which WaveLAN protocol is being sent. The last frame of the SNAP model is the WaveLAN higher protocol message that contains information that varies between protocols and can contain between 38 and 1492 bytes of information.

5.5 The PtPMeasure Protocol

The PtPMeasure protocol was developed by Lucent Technologies for making measurements of the signal level (*SL*) and signal-to noise-ratio (*SNR*). The signal level is

WaveLAN MAC Frame

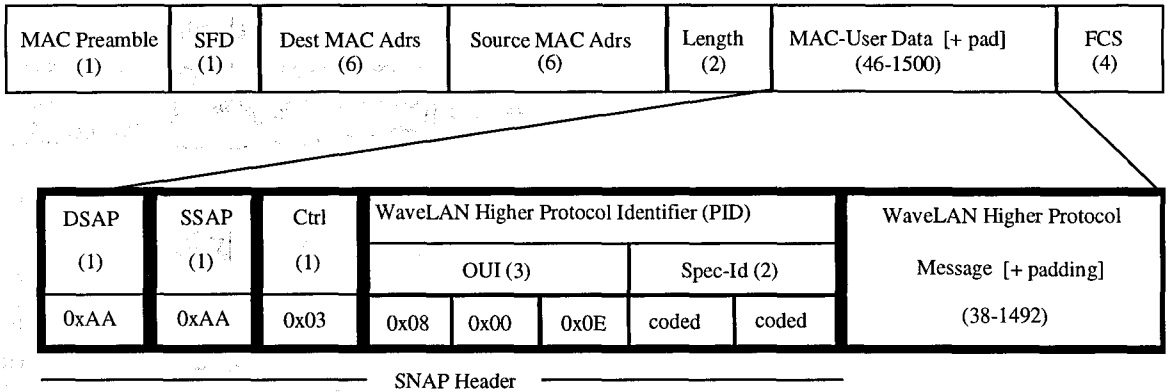


Figure 5.3 SNAP frame structure

Reprinted from: Leo Monteban and Henri Moelard, "Data Manual: WaveLAN Air Interface", © 1997 AT&T

an 8-bit word that is read from the RF-modem and ranges from a minimum of 0 decimal to a maximum of 36 decimal (0 to 24 hexadecimal). The *SNR* that is given by the PtPMeasure program is calculated using the mean signal level (*SL*) and mean noise level (*NL*) where the *NL* is simply the signal level output of the RF-modem during periods of RF silence and mean refers to an average of the past five values. The *SNR* is given by :

$$SNR = SL - NL \quad (5.1)$$

thus the range of the *SNR* is -36 to 36 decimal, although negative *SNR* values are treated as zero. The *SNR* is expressed as a difference rather than a ratio due to the linear relationship between the values given by the PtPMeasure program and the received power in dBmW.

The PtPMeasure request frame structures are shown in Figure 5.4. The request frames, PtPMeasure-REQ/1 and PtPMeasure-REQ/2, are sent in sequence from the station that is requesting information about the transmission quality of its signal. The first two frames shown are the WaveLAN specific ID codes of the SNAP model. The first field contains the value 20 hexadecimal and the second contains the value 02 hexadecimal . These values indicate to the receiver that this is a diagnostic protocol. The protocol data unit (PDU) frame contains the value 03 hexadecimal which further identifies the packet as a PtPMeasure packet. The variant field identifies the protocol variant used by the requester to the responder. The sequence frame contains a value that increments by one every time a

PtPMeasure-REQ/1

WaveLAN Specific ID (2)	PDU Type (1)	Variant (1)	Sequence (1)	RSP-length (2)	Padding (33)
0x20	0x02	0x03	coded	coded	don't care

PtPMeasure-REQ/2

WaveLAN Specific ID (2)	PDU Type (1)	Variant (1)	Sequence (1)	RSP-length (2)	Padding (34 - 1487)
0x20	0x02	0x03	coded	coded	don't care

Figure 5.4 PtPMeasure request frames

Reprinted from: Leo Monteban and Henri Moelard, "Data Manual: WaveLAN Air Interface", © 1997 AT&T

new request packet sequence is sent and is used by the responder to differentiate between request frames. The RSP-length field contains the requested value of the total MAC frame (excluding the FCS) of the PtPMeasure-RSP/2 frame. The padding field of the PtPMeasure-REQ/1 frame contains 33 bytes of arbitrary data while the padding field of the PtPMeasure-REQ/2 frame contains between 34 and 1487 bytes.

The PtPMeasure response frames are shown in Figure 5.5 The ID, PDU, variant, and sequence fields have the same meaning as for the request frames. The RF-attributes field contains 3 bytes of information about the requesters signal level and noise level. As it was for the request frames, the length of the padding field is the only difference between PtPMeasure-RSP/1 and PtPMeasure-RSP/2 frames.

5.6 Signal Level and SNR Calculations

The PtPMeasure user interface displays signal level (SL) and signal-to-noise (SNR) ratio measurements on a scale from 0 to 100 percent. The output signal level value given by the RF modem ranges from 0 to 36 decimal and the displayed value on the user interface is calculated as [20]:

$$SL_{Displayed} = 3 \cdot (SL_{RF \text{ Modem}}) \quad (5.2)$$

PtPMeasure-RSP/1

WaveLAN Specific ID (2)	PDU Type (1)	Variant (1)	Sequence (1)	Status (1)	RF-Attributes (3)	Padding (31)
0x20	0x02	0x04	coded	coded	coded	don't care

PtPMeasure-RSP/2

WaveLAN Specific ID (2)	PDU Type (1)	Variant (1)	Sequence (1)	Status (1)	RF-Attributes (3)	Padding (32 - 1485)
0x20	0x02	0x04	coded	coded	coded	don't care

Figure 5.5 PtPMeasure response frames

Reprinted from: Leo Monteban and Henri Moelard, "Data Manual: WaveLAN Air Interface", © 1997 AT&T

Where displayed signal levels that are greater than 100 are set to 100. The SNR is calculated as given by Equation (5.1). The signal level output by the RF modem versus the received power in units of dBmW is shown in Figure 5.6. Although the PtPMeasure user interface does not display the received noise level, by knowing the signal level and SNR it can be calculated by arranging Equation (5.1) as:

$$NL = SL - SNR \quad (5.3)$$

The received noise power can be determined from the relationship between the signal level given by the RF modem and power in dBmW shown in Figure 5.6

5.7 Library Architecture

There are two different types of walls used in the area where propagation measurements were made in the library. The first, designated W4 by the architect, has a total thickness of 15.6 cm and consists of two layers of 1.6 cm sheet rock (gypsum board) on each side with 6.4 cm of acoustic insulation within the wall. The second, designated W3, has a total thickness of 12.4 cm and consists of one layer of 1.6 cm sheet rock (gypsum board) on each side with 6.4 cm of acoustic insulation within the wall. Both types of walls have steel metal studs placed 40.6 cm apart. The first and second floors are separated by 25 cm of steel reinforced concrete as are the second and third floors.

Signal Level / dBm relation at 2.4 GHz

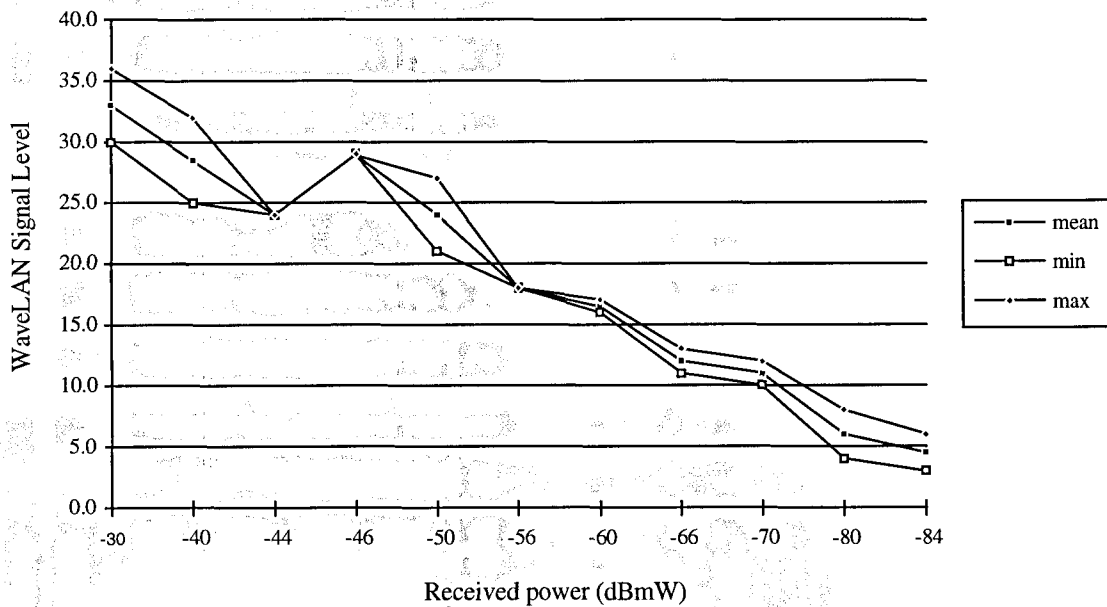


Figure 5.6 RF modem signal level vs. received power

Reprinted from: Loeke Brederveld and Henri Moelard, "WaveLAN Signal Strength and S.N.R. calculations", © 1995 AT&T

5.8 Measurements

Measurements of signal strength and signal-to-noise ratio were made at various locations on the first, second, and third floors of Hodges Library. Figures 5.7, 5.8, and 5.9 are enlarged views of the first, second, and third floors with measurement points denoted by numbers. All measurements were taken at a height of 75 cm above the floor which is a typical height for a desktop where a laptop computer is likely to be positioned.

For unobstructed line-of-sight transmission, the received power decays as a function of the transmitter-receiver separation distance as given by the Friis free space equation which is given by [18]:

$$P_r(d) = \frac{P_t G_t G_r \lambda^2}{(4\pi)^2 d^2 L} \quad (5.4)$$

Where P_t is the transmitted power, $P_r(d)$ is the received power as a function of the transmitter-receiver separation distance, G_t is the transmitter antenna gain, G_r is the receiver antenna gain, d is the distance between the transmitter and receiver, L is the system loss not related to propagation ($L \geq 1$), and λ is the wavelength in meters. However since Equation (5.4) is undefined for $d = 0$, propagation models use what is known as a close-in distance, d_o , as a known receiver reference point [18]. For the power

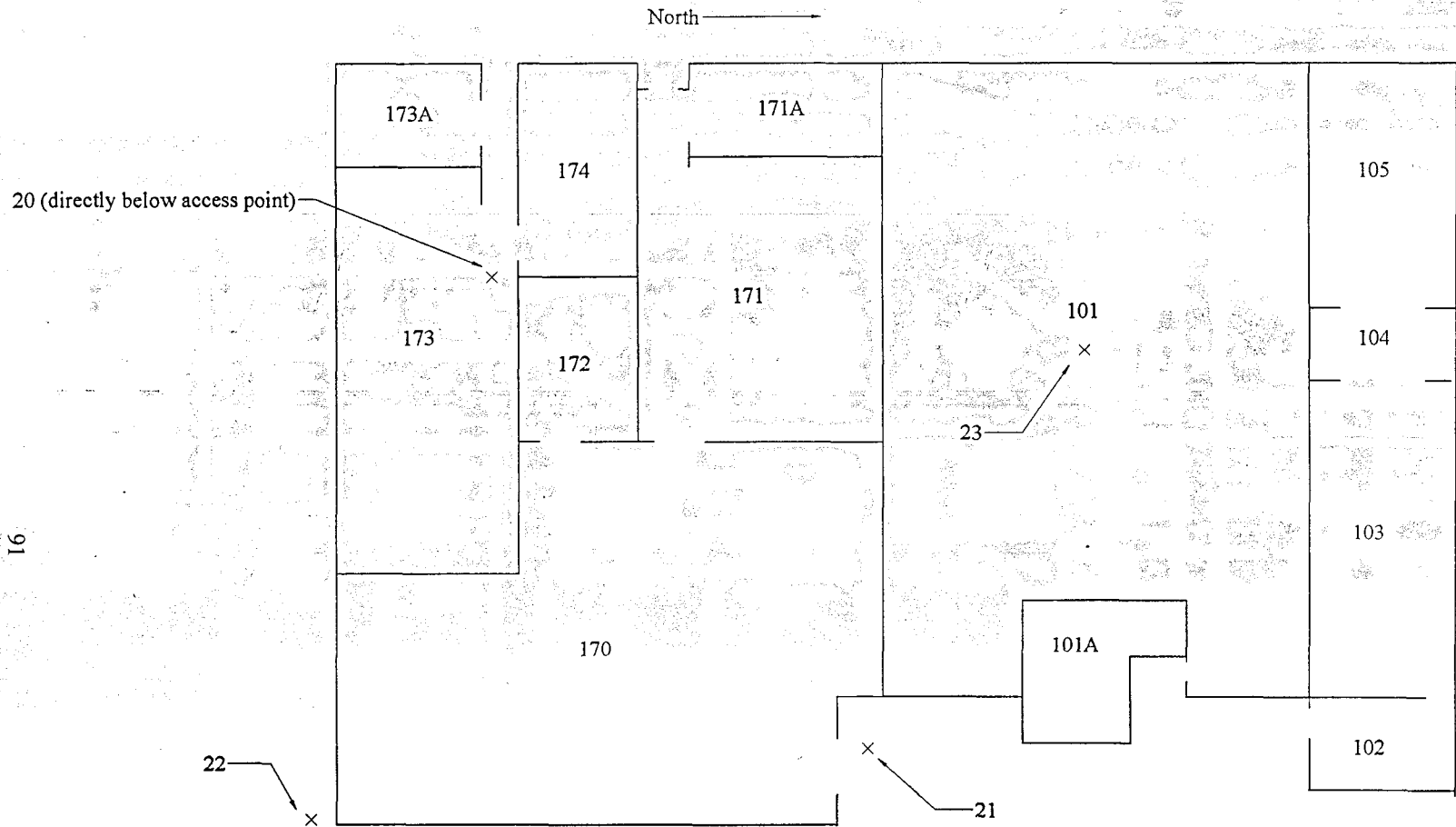


Figure 5.7 First floor measurement locations

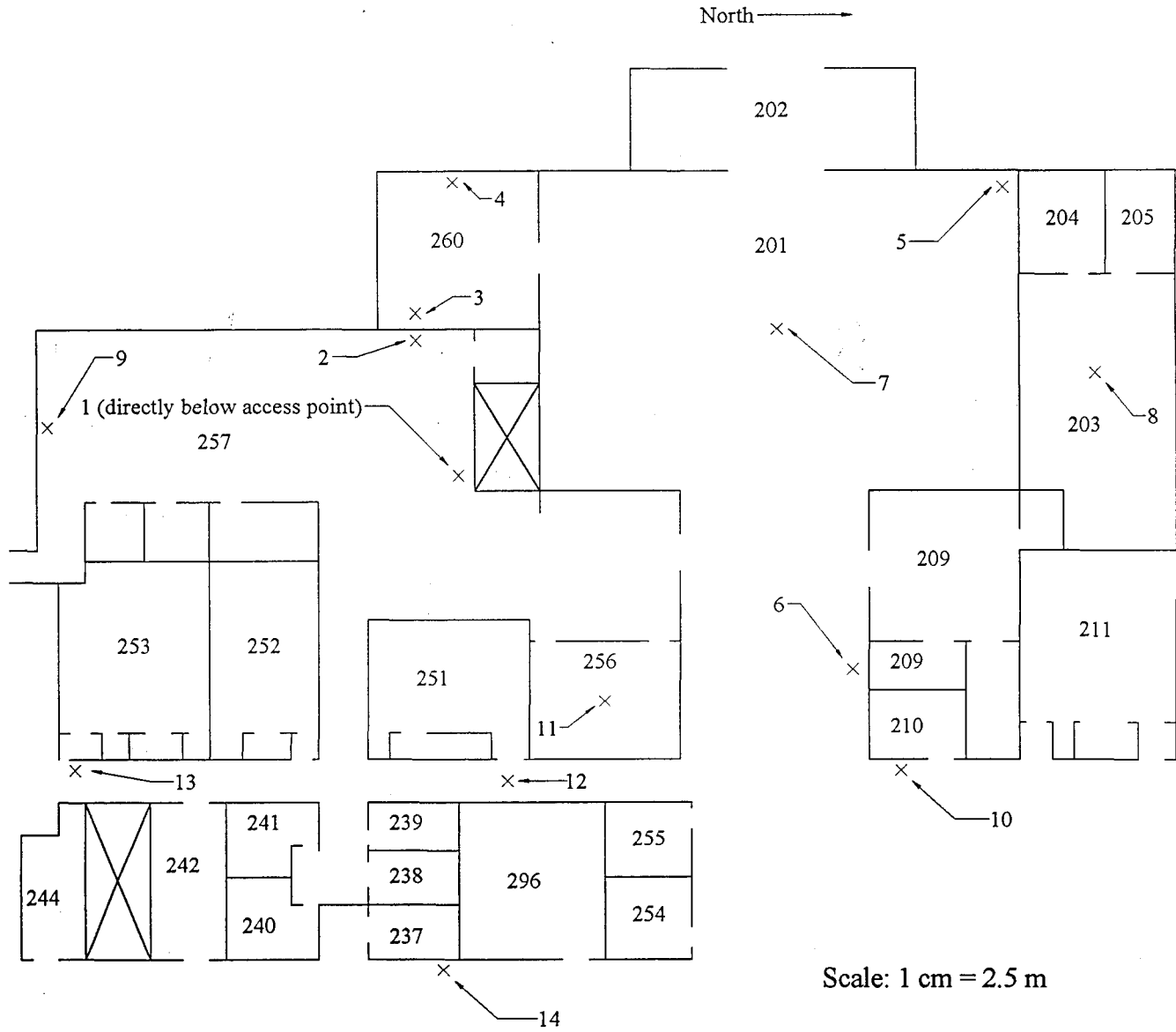


Figure 5.8 Second floor measurement locations

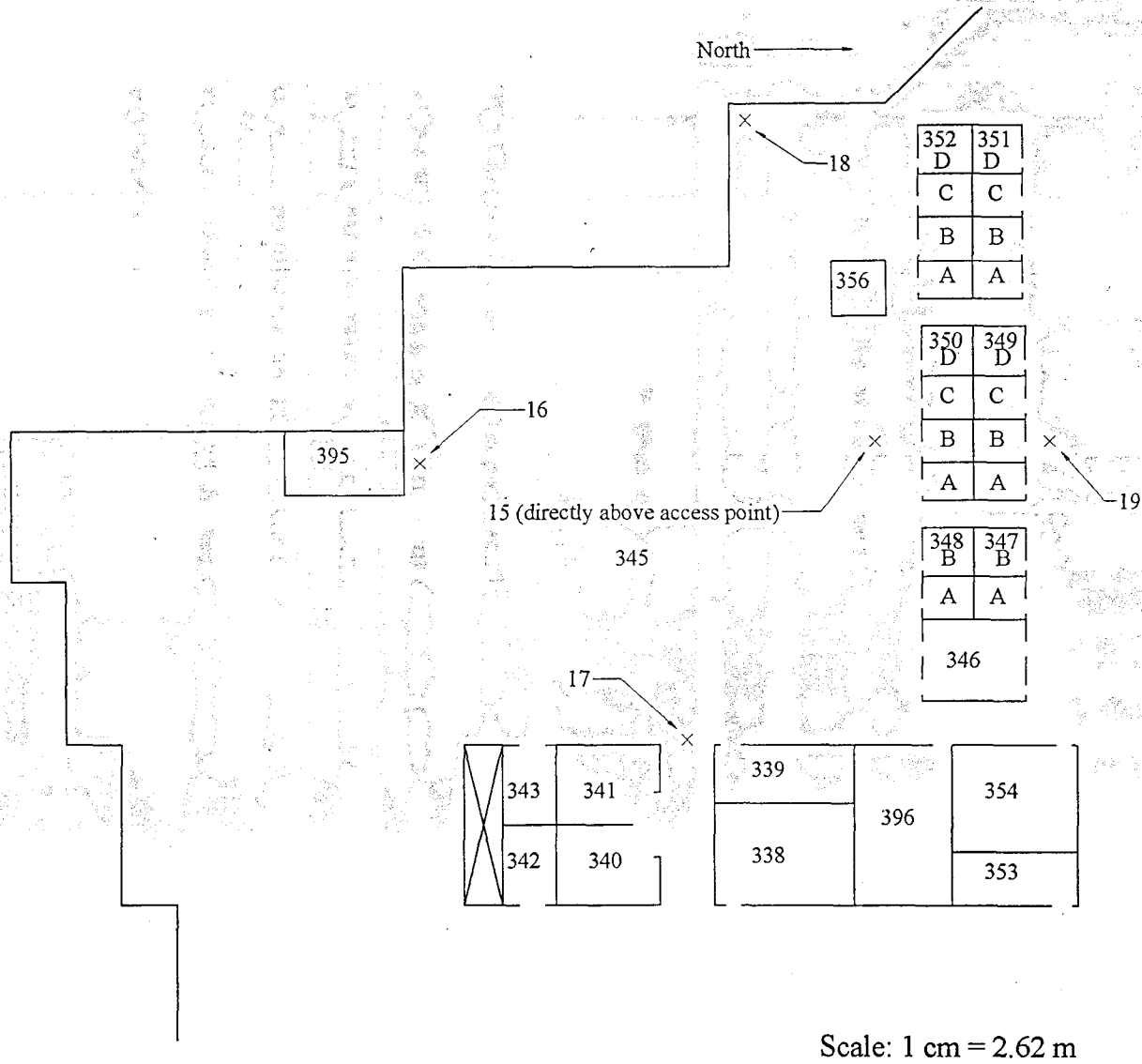


Figure 5.9 Third floor measurement locations

measurements shown in Figure 5.6, $d_o = 1$ meter which is typical for indoor propagation measurements at high frequencies.

Equation (5.4) can be used to relate the received power in free space at a distance greater than d_o as:

$$P_r(d) = P_r(d_o) \left(\frac{d_o}{d} \right)^2 \quad d \geq d_o \quad (5.5)$$

which can be expressed in units of dBmW by taking the logarithm of both sides and multiplying by 10. Thus in units of dBmW, the received power is given by:

$$P_r(d) = 10 \log \left[\frac{P_r(d_o)}{.001} \right] + 20 \log \left(\frac{d_o}{d} \right) \quad d \geq d_o \quad (5.6)$$

However, indoor environments usually have partitions which also effect the propagation characteristics. A common expression used to estimate the path loss (PL) in an indoor environment is given by:

$$PL(dB) = PL(d_o) + 10n \log \left(\frac{d}{d_o} \right) + X_\sigma \quad (5.7)$$

where the value of n depends on the surroundings and building type, and X_σ is a Gaussian random variable in dB having a standard deviation of σ dB. Table 5.1 shows values of n and σ which have been measured in different buildings [18]. Equations (5.6) and (5.7) can be combined to yield the received power in an indoor environment in dBmW as:

$$P_r(d) = 10 \log \left[\frac{P_r(d_o)}{.001} \right] + 10n \log \left(\frac{d_o}{d} \right) + X_\sigma \quad d \geq d_o \quad (5.8)$$

Using the known value of $P_r(d_o)$ from Figure 5.6, Equation (5.8) can be written for the WaveLAN system as:

$$P_r(d) = -30 + 10n \log \left(\frac{d_o}{d} \right) + X_\sigma \quad d \geq d_o \quad (5.9)$$

The WaveLAN access point is positioned above the ceiling tile on the second floor 375 cm above the floor which is 300 cm (3 m) above the plane where the measurements on the second floor were taken. Thus for measurements taken on the second floor of the library, the distance between the access point and laptop can be calculated by using the constant vertical distance, $d_v = 3$ m, and the horizontal distance, d_h , which can be measured from the floor plan as:

$$d = \sqrt{(d_v)^2 + (d_h)^2} \quad (5.10)$$

Table 5.1 Path loss exponent and standard deviation for various types of buildings

	n	σ (dB)	Number of locations
All Buildings:			
All locations	3.14	16.3	634
Same Floor	2.76	12.9	501
Through One Floor	4.19	5.1	73
Through Two Floors	5.04	6.5	30
Through Three Floors	5.22	6.7	30
Grocery Store	1.81	5.2	89
Retail Store	2.18	8.7	137
Office Building 1:			
Entire Building	3.54	12.8	320
Same Floor	3.27	11.2	238
West Wing 5th Floor	2.68	8.1	104
Central Wing 5th Floor	4.01	4.3	118
West Wing 4th Floor	3.18	4.4	120
Office Building 2:			
Entire Building	4.33	13.3	100
Same Floor	3.25	5.2	37

Reprinted from: Theodore S. Rappaport, "Wireless Communications: Principles & Practice", Prentice Hall, New Jersey, 1996.

for the third floor of the library, d_v is approximately 1 m and for the first floor, d_v is approximately 7.75 m.

Table 5.2 shows the site location, transmitter-receiver distance, received signal power, signal-to-noise ratio (SNR), and calculated n for the measurements taken on the second floor of Hodges Library. The exponent n was obtained by solving Equation 5.9 for n and assuming $X_\sigma = 0$ (its mean value) as:

$$n = \frac{P_r(d) + 30}{10 \log \left(\frac{d_o}{d} \right)} \quad (5.11)$$

and then substituting the measured values of d and $P_r(d)$. Tables 5.3 and 5.4 contain the propagation data for the third and first floors of the library, respectively. By using Equation (5.3), the received noise power was found to be relatively constant at -88 dBmW. Thus the SNR is always equal to the value of the received power plus 88 dBmW.

From the data in Table 5.3 it can be seen that for locations where a line-of-sight path exists between the transmitter and receiver (i.e., site locations 1, 2, and 9) that n is approximately equal to 2 and thus the Friis free space equation is obeyed. For the other second floor locations, n is typically closer to 3 which is due to obstructions in the signal path. Signal attenuation is more severe for the third and first floors, with n approximately equal to 4. Table 5.5 shows the mean n and standard deviation between measured and

predicted path loss (using the mean value of n) for each floor in a similar fashion as Table 5.1.

Table 5.2 Propagation data for the second floor of Hodges Library

Site Number	T-R distance (meters)	Received Power (dBmW)	S.N.R. (dB)	n
1	2.0	-36	58	2.0
2	5.8	-44	44	1.8
3	6.8	-55	33	3.0
4	10.6	-59	29	2.8
5	23.0	-70	18	2.9
6	18.0	-59	29	2.3
7	14.0	-64	24	3.0
8	25.9	-78	10	3.4
9	15.5	-54	34	2.0
10	22.0	-70	18	3.0
11	11.1	-60	28	2.9
12	13.0	-62	26	2.9
13	18.5	-70	18	3.2
14	20.5	-80	8	3.8

Table 5.3 Propagation data for the third floor of Hodges Library

Site Number	T-R distance (meters)	Received Power (dBmW)	S.N.R. (dB)	n
15	4.0	-54	34	4.0
16	15.0	-80	8	4.3
17	12.0	-70	18	3.7
18	12.0	-70	18	3.7
19	6.7	-70	18	4.8

Table 5.4 Propagation data for the first floor of Hodges Library

Site Number	T-R distance (meters)	Received Power (dBmW)	S.N.R. (dB)	n
20	7.75	-64	24	3.8
21	14.3	-78	10	4.2
22	14.3	-80	8	4.3
23	16.4	-83	5	4.4

Table 5.5 Path loss exponent and standard deviation data for Hodges Library

	n	σ (dB)	Number of locations
All locations	3.3	6.2	23
Second floor	2.8	7.0	14
Third floor	4.1	4.7	5
First floor	4.2	3.8	4

5.9 Evaluation of Data

Lucent Technologies defines a minimum acceptable SNR (as read from the RF modem) as 9 which corresponds to a signal level of -70 dBmW. This was also the observed signal level threshold where operation became unreliable while taking measurements. By solving Equation (5.9) for d as:

$$d = \frac{d_o}{10^{\frac{P_r(d)+30-X_\sigma}{10n}}} \quad (5.12)$$

and substituting -70 dBmW for $P_r(d)$, 1 m for d_o , and letting X_σ equal its average value of 0 , the approximate maximum transmitter-receiver distance can be obtained for a given n . For the second floor of the library where $n = 2.8$, the corresponding maximum distance is $d_m = 34.3$ m. For the first and second floors where n is approximately equal to 4.2 , the maximum T-R separation is 10.6 m.

The signal-to-noise ratio referred to in this chapter is the ratio of received signal power, P_r , to the received noise power, N . In Chapter 4, the signal-to-noise ratio was defined as the ratio of the energy per symbol, E_s , to the single sided noise power spectral density, N_o (the noise power in a 1 Hz bandwidth.) The following relationships exist between the aforementioned parameters [4]:

$$N_o = \frac{N}{W} \quad (5.13)$$

$$P_r = E_s R \quad (5.14)$$

where W is the bandwidth of the receiver and R is the symbol rate. The symbol rate for the WaveLAN system is 11 MHz, and for a double-sideband (DSB) DQPSK system the required bandwidth is $2R = 22$ MHz. Using Equations (5.13) and (5.14):

$$\begin{aligned} \frac{P_r}{N} &= \frac{E_s R}{N_o W} \\ &= \frac{E_s}{2N_o} \end{aligned} \quad (5.15)$$

thus the power SNR used in this chapter is simply twice (3 dB greater than) the SNR as defined in Chapter 4.

As stated in Section 5.8, the measured noise power was relatively constant as -88 dBmW. Since the minimum acceptable signal level was found to be -70 dBmW, this yields a minimum power SNR of $-70 - (-88) = 18$ dB which corresponds to an energy SNR of 15 dB using Equation (5.15). Assuming no multipath interference, this corresponds to a symbol error rate (see Figure 4.25) of 4×10^{-5} or a bit error rate (using Equation (4.8)) of 2×10^{-5} .

A full WaveLAN MAC frame consists of 1,520 bytes, or 12,160 bits. For a given bit error probability, the probability of receiving one bit of a frame incorrectly can be computed using the Poisson approximation to the binomial distribution[15]. The approximation is given by:

$$P_e(f) \cong 1 - e^{-np} \quad (5.16)$$

where $P_e(f)$ is the probability of receiving one or more bits incorrectly in one frame, p is the probability of bit error, and n is the number of bits in each frame. Using $p = 2 \times 10^{-5}$ and $n = 12,160$:

$$P_e(f) \cong 1 - e^{-(12160)(0.00004)} = 0.21 \quad (5.17)$$

thus at the threshold SNR for acceptable performance, approximately 2 out of 10 transmitted frames are received in error and thus must be retransmitted.

Chapter 6

Conclusion

The first three chapters of this thesis provided useful background information concerning current wireless LAN technology available for use in the United States. In the future, wireless LANs that will support higher data rates are expected to appear on the scene. In Europe, the high-performance radio LAN standard (HIPERLAN) is being developed which will allow data rates up to 23 Mbits/s using the 5.3 GHz band. Higher data rates than are currently available will be necessary for wireless LANs to support video quality and multimedia transmissions which require greater bandwidth.

Chapter 4 demonstrated the DQPSK DS/SS transmission process used by the WaveLAN system. It was shown that the use of DS/SS significantly increases the error performance of the system when multipath interference is present.

For future implementations of wireless LANs on the University of Tennessee campus, Chapter 5 should serve as a useful guide in determining the coverage area of an access point. For Hodges Library, it was shown that a radius of approximately 34 meters can be covered by one access point. The coverage area was significantly smaller between floors, so it is not recommended that the system be used for between-floor applications in Hodges Library. For other architectures that differ in composition, Chapter 5 can be used as a guide to determine the number of access points necessary.

List of References

List of References

- [1] Orichi-Batajolo, Aquilino B., "Performance of a Frequency Hop Spread Spectrum Multiple Access Radio Network in a Factory Environment", Master of Science Thesis in Electrical Engineering, The University of Tennessee, Knoxville, August, 1994.
- [2] Davis, Peter T., McGuffin, Craig R., "Wireless Local Area Networks", McGraw-Hill, Inc., New York, 1994.
- [3] Tuch, Bruce, "Development of WaveLAN, an ISM Band Wireless LAN", AT&T Technical Journal, July/August, 1993.
- [4] Sklar, Bernard, "Digital Communications; Fundamentals and Applications", Prentice Hall, New Jersey, 1988.
- [5] Muller, Nathan J., "Wireless Data Networking", Artech House, Inc., 1995
- [6] Wickelgren, Ingrid J., "Local Area Networks go Wireless", IEEE Spectrum, September 1996.
- [7] Bennington, Ben, "Report on Progress in Implementing a High Speed Wireless Infrastructure", Carnegie Mellon University, August 1996.
- [8] Miller, Mark, "LAN Protocol Handbook", M&T Publishing, 1990
- [9] Moelard, Henri, "WaveLAN Spread Spectrum Techniques", WaveLAN Technical Note, ©AT&T, September, 1994.
- [10] Davidson Hugh, van der Moolen, William, "WavePOINT Installation and Operation Guide", ©AT&T, 1995.
- [11] Moelard, Henri, "WaveLAN Security" WaveLAN Technical Note, ©AT&T, September, 1994.
- [12] Stone, Charles, "The Data Encryption Standard: an Update", NIST Special Publication 800-2, Public Key Cryptography, 1995.
- [13] Davidson, Hugh, "WaveLAN/PCMCIA Card Users Guide", 1995.

- [14] Ziemer Rodger E., Peterson, Roger L., "Digital Communications and Spread Spectrum Systems", Macmillan Publishing Company, New York, 1985.
- [15] Ziemer, Rodger E., Tranter, W.H., "Principles of Communications: Systems, Modulation, and Noise", Houghton Mifflin Company, Boston, 1990.
- [16] Prabhu, Vasant K., "Error Rate Bounds for Differential PSK", IEEE Transactions on Communications, December 1982.
- [17] Hashemi, Homayoun, "Impulse Response Modeling of Indoor Radio Propagation Channels", IEEE Journal on Selected areas in Communications, September, 1993.
- [18] Rappaport, Theodore S., "Wireless Communications: Principles & Practice", Prentice Hall PTR, New Jersey, 1996.
- [19] Fielhauer, Karl B., "Using RF Channel Simulators to Test New Wireless Designs", RF Magazine, January 1994.
- [20] Moelard, Henri, Brederveld, Loeke, "Wireless Connection I/F Design Note", ©AT&T, 1995.
- [21] "LabVIEW 3.1 User Manual", National Instrument Corporation, Austin, Texas, 1994.

Vita

John P. Parsley was born in Owensboro, Kentucky on January 9, 1967. He graduated from Apollo High School in 1985. In May, 1990, he entered the University of Tennessee and graduated Magna Cum Laude with the Bachelor of Science in Electrical Engineering in December 1993. In January 1995, he was admitted to the University of Tennessee graduate school to pursue a Master of Science degree in Electrical Engineering, and received his Master of Science Degree in Electrical Engineering in May, 1997.